Geo-information Science and Remote Sensing

Thesis Report GIRS-2023-20

Assessing Water Stress in Maize Using UAV Thermal Infrared Sensing

Marta Nidola

18/04/2023

WAGENINGEN
UNIVERSITY & RESEARCH

Assessing Water Stress in Maize Using UAV Thermal Infrared Sensing

Marta Nidola

Registration number 1164228

<u>Supervisors</u>:

Magdalena Smigaj
Quanxing Wan

A thesis submitted in partial fulfilment of the degree of Master of Science
at Wageningen University and Research,
The Netherlands.

18/04/2023
Wageningen, The Netherlands

Abstract

Crop water stress (CWS) caused by inadequate soil moisture content (SMC) is a major factor affecting agricultural productivity. Remote sensing technologies, such as thermal infrared (TIR) cameras on Unmanned Aerial Vehicles (UAVs), offer a potential solution for monitoring CWS. In this study, the relationships between canopy temperature (T_c) obtained from UAV-based TIR data and ground measurements of SMC, plant water content (PWC), and dried leaves weight (DLW) were investigated to support the use of TIR for CWS detection. Two different soil-pixel exclusion methods using the Otsu algorithm and Normalized Difference Vegetation Index (NDVI) thresholding were compared, and the influence of cover crops on UAV-ground measurement relationships was assessed. The study focused on maize at three different growth stages after six years of winter cover crop use, hypothesizing cover crops impact these relationships. The findings revealed a correlation between T_c and PWC and DLW (r=-0.45*/-0.67***, and -0.19**/-0.58***, respectively), suggesting T_c could serve as a proxy for crop water status. However, T_c was not effective in estimating SMC. In this relation, the cover crop represented by the grass species "oat" may have led to unfavourable conditions for maize that resulted in lower PWC and biomass than other treatments ($p < 0.05$). Furthermore, the performance of the Otsu algorithm varied depending on the maize growth stage, which affected its applicability. Overall, the study highlighted the challenges and opportunities associated with thermal imaging for CWS monitoring, emphasising the importance of data interpretation. Further research is needed to explore the relationship between T_c and SMC with the inclusion of NDVI as a normalization factor and to better understand the impact of long-term cover crops on the SMC in no-tillage conditions.

Keywords: remote sensing, canopy temperature, thermography, UAV, crop water stress, maize, soil moisture content, cover crops.

Table of contents

List of Abbreviations:

CWS = Crop Water Stress
DFW = Dried Fruit Weight
DLW = Dried Leaves Weight
DN = Digital Number
ExG index = Excess Green index
Gs = stomatal conductance
LST= land surface temperature
NDVI = Normalised Difference Vegetation Index
PSF = Plant-Soil Feedback
PWC = Percentage of Water in the leaves
RGB = Red Green Blue wavelengths
sdT_c = standard deviation of canopy temperature
SNR = Signal to Noise Ratio
SOC = Soil Organic Carbon
SOM = Soil Organic Matter
SMC = Soil Water or Soil Moisture Content
SWD = soil water deficit
T_c = canopy temperature
TIR = thermal infrared
TVDI = temperature vegetation dryness index
UAV = Unmanned Aerial Vehicles

1 Introduction

1.1 Context and background

Crop water stress, which is defined as water deficiency in the soil for crop use, represents a problem for farmers since plant growth may be undermined in the long term, leading to overall decreased productivity (Gerhards et al., 2019). Therefore, techniques for water stress monitoring are of the utmost importance. Currently, techniques for the detection of water stress in crops rely on direct measurements of the soil water content or assessment of physiological and biophysical changes occurring in crops (Ekinzog et al., 2022).

In recent years, with advancements in technology, imagery of plant or canopy temperature (T_c) using UAV-mounted thermal infrared (TIR) cameras started being explored due to its ability to offer a more complete picture of the spatial variability of crop water status compared to ground measurements (Messina and Modica, 2020). With TIR data collected by Unmanned Aerial Vehicles (UAVs), the workload in the field can be minimized. However, issues linked to the limitations of TIR cameras are introduced and need to be tackled with procedures that correct for the sensor's intrinsic characteristics and ambient environmental conditions (Kelly et al., 2019). Given that, protocols known to derive accurate temperature data have been developed and methods for T_c extraction have been proposed (Jones and Sirault, 2014; Kelly et al., 2019).

Nonetheless, using thermal imaging for monitoring purposes is further complicated by the fact that T_c is not only influenced by soil water content. Another potential way for controlling T_c is through biomass growth, as increased foliage leads to higher evapotranspiration and lower T_c (Ekinzog et al., 2022). For example, as biomass grows, a confounding effect in the relation between soil water content and T_c is introduced. On the other hand, the isolated influence of canopy structural parameters, which are for example represented by the biomass allocation to leaves and stems, can be seen later in the phenological stages, when at physiological maturity the canopy is not transpiring anymore (Anderegg et al., 2021). The link between T_c and soil water content, which reflects plant water status, was established long ago. Since then, TIR images have been helping to drive irrigation strategies aimed at decreasing T_c through an increase in soil water content via irrigation (Ekinzog et al., 2022; Gerhards et al., 2019). However, sustainable agricultural practices claim that water-use efficiency can be not only achieved with punctual water inputs but also by encouraging mechanisms for water retention and decreased loss. One of the mechanisms is cover crop use. The purpose behind the cultivation of cover crops is to benefit from their influence on soil properties, which the following plants can take advantage of (Blanco-Canqui and Ruis, 2020). This concept is called plant-soil feedback (PSF). Cover crops were found to affect the soil structure through improved water infiltration and absorption, as well as soil fertility by improving nutrient retention and cycling (Blanco-Canqui and Ruis, 2020; Daryanto et al., 2018; Koudahe et al., 2022).

To add complexity, these two benefits of PSF need different duration of cover crop use to become explicit; additionally, different cover crops are reported to impact them differently (Blanco-Canqui and Ruis, 2020; Hunter et al., 2021).

1.2 Problem definition

The UAV-derived T_c serves for crop water stress monitoring, and water in the soil is the interest around which the study revolves, as it can be targeted efficiently and timely to reduce T_c (Zhang et al., 2019). A significant correlation between soil moisture in the first 40 cm depth and Crop Water Stress Index (CWSI) is reported in the study by Ru et al. (2020). As T_c, CWSI has a strong relationship with the plant water status indicators, but differently from T_c, CWSI requires an artificial setup with an irrigation scheme, which is often difficult to set

at the field level. Therefore, the choice of T_c lies in its simplicity and the fact Zhang et al. (2019) reported that it is an effective indicator of water stress in maize that it is better able to reflect the status of soil water content at shallow root zone depths (20 cm), typical of this crop. Because of its importance, the effect of soil water content on T_c measured with UAV must be evaluated. Moreover, it has to be verified if the relation between soil water content and T_c is maintained during the growing season. Existing literature focused on examining the relation on a single acquisition day at different soil depths for exploring the water uptake zone for maize (Zhang et al., 2019). While having this relationship confirmed for different crop stages with soil water content sampled at 20 cm would mean that remote sensing techniques with their advantages over ground measurements could gather information needed on the water in the soil, and T_c could be used as a proxy for plant status (Messina and Modica, 2020). However, given the confounding effect of biomass and soil water content on T_c, it becomes important to distinguish which influences the T_c the most at the field level and to separate the two during the crop growth to see if the strength of the relationship is maintained over the growing season. This research represents a novelty in the sense that existing literature has focused on determining the causative relation between crop water stress and the consequently reduced biomass growth rather than the influence of biomass on T_c (Li et al., 2019; Song et al., 2019). Furthermore, some studies investigated other canopy aerodynamic characteristics such as roughness and crop height (Gerhards et al., 2019; Prashar and Jones, 2014), but so far no research focused on the influence of biomass on the canopy energy balance.

Biomass accumulation and soil water content, and consequently T_c may be affected by the PSF after cover crops. The existing literature about cover crops suggests that their short-term use associated with tillage repeated for a few years has the potential to increase macropores' presence (Haruna et al., 2023), which however is not reported to bring benefits in terms of soil hydraulic properties (Hunter et al., 2021). The effect on soil water content for long-term studies on the cover crop is only documented in the case of no-tillage practices. For prolonged cover crop use and no-tillage, Araya et al. (2022) report an improvement in soil structure accompanied by increased water retention. Nonetheless, little is known about whether tillage's positive effects on macropores may persist over time when combined with a cover crop grown in succession for several years. Therefore, a study on the long-term use of cover crops of different types associated with ploughing becomes relevant. Assessment of cover crop performances when compared to the control (fallow) could highlight a difference in soil water content, besides the expected biomass variations already reported in the literature due to the fertilizing properties of cover crops (Fageria et al., 2005). Cover crops have to be studied individually by measuring the soil water content and biomass of the following cash crop. The use of T_c could help evaluate the effects of different cover crops and shed light on important benefits on soil hydraulic properties due to their long-term use, however, it is unclear if (and how) the use of different cover crops affects the relationship between canopy temperature and soil water content.

For the achievement of thermal observations with the temporal and spatial scales more suitable to the study, UAV is generally deployed because of its flexibility in timing and flight height (Delavarpour et al., 2021). However, as it occurs with satellite or airborne images, further steps for obtaining T_c are to be undertaken and these depend on the method used for T_c extraction. The choice of the method used for removing soil from the pixels still constitutes a determinant passage that affects the overall thermal map and the results (Jones and Sirault, 2014). Besides a routinely used method based on NDVI, more sophisticated approaches such as the Otsu algorithm have been studied and shown promising results (Jones and Sirault, 2014; Zhang et al., 2019). Zhang et al. (2019) demonstrated that T_c extracted by the Otsu method is highly correlated with the ground-truth measurements with R^2 of 0.94 (n = 15) and RMSE of 0.7°C, and therefore representing the T_c with high accuracy. Decisions on which methods to use need to be drawn according to the achievable accuracy in removing soil pixels.

1.3 Overall research aim and research questions

The main aim of this thesis is to assess whether UAV thermal data can be used to obtain information about soil water content which is a proxy of crop water status and to determine to what extent biomass and soil water content derived from ground measurements are responsible for T_c changes obtained from the thermal camera on a UAV. Secondly, the effects of cover crops on this relationship will be investigated. To address this aim, three research questions will be answered. The first research question evaluates the performance of the background soil removal methods. The second and the third research questions focus on exploring the relation between UAV-derived T_c with soil water content and structural parameter as biomass at the field and plot level respectively during the growing season of maize.

To execute the above-mentioned aim, the following research questions are set up:

RQ1: Which soil background removal method performs best at different maize growth stages?

RQ2: What is the relationship between T_c, biomass, and soil water content and how can the ground measurements of the last two help to interpret the thermal data of maize crops?

RQ3: How do cover crops influence the interrelation of soil water content, maize T_c and biomass?

2 Material and Methods

2.1 Study site and Experimental Design

This study was conducted in a 1.21 ha research field (Latitude 51.995123 Longitude 5.660100), located 500 meters north of the Wageningen University and Research campus, the Netherlands, during the summer of 2022 (Figure 1 A). The study field was divided into five blocks with eight plots each (Figure 1 B). Within a block, each plot, whose dimensions were 10 m x 6 m, was randomly assigned one of the eight selected cover crop treatments. The treatments consisted of different species of cover crops, which have been grown in the same location every winter since 2016: oat (Avena strigosa, abbreviated as "O" in the text), radish (Raphanus sativus – "R") and vetch (Vicia sativa – "V"), bi- or tri-species mixtures ("VO", "VR", "OR" and "VOR" with mixing ratios of 50:50 and 33:33:33); one control plot was the fallow treatment ("F" in the text).

A

B
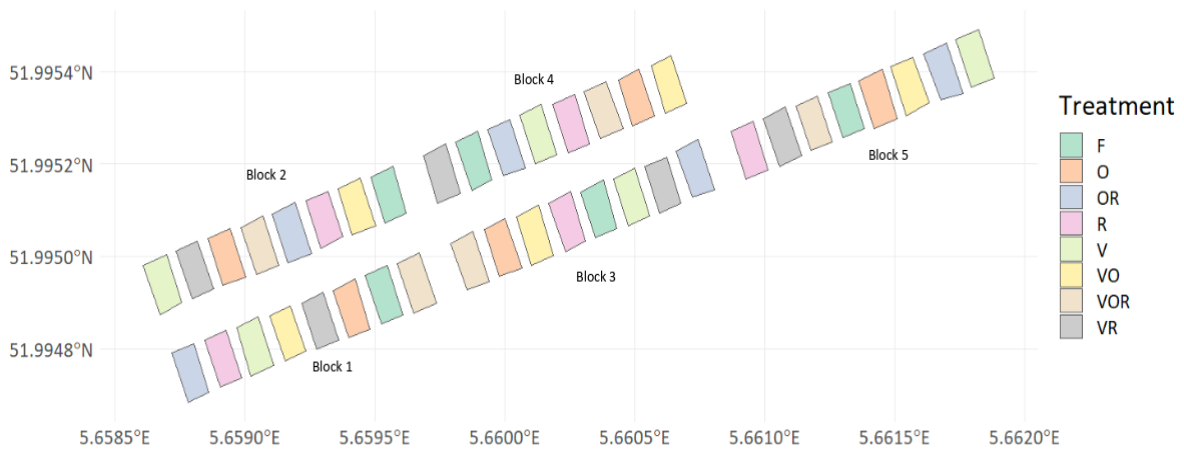
Figure 1 A Location of the study area with zoom into the field level (RGB orthomosaic derived from DJI Matrice 210 (RTK) on 09/08/2022) and Figure 1 B distribution of cover crop types in the blocks. Abbreviations: oat (Avena strigosa – "O"), radish (Raphanus sativus – "R") and vetch (Vicia sativa – "V"), bi- or tri-species ("VO", "VR", "OR" and "VOR"); fallow ("F").

After cover crops, the cash crop of the year was grown. Although soil texture was reported to be of one type only and defined as sandy (B2) according to the Dutch system of soil classification (Heinen et al., 2022), soil sampling in November 2021 (Appendix I) demonstrated that there is a soil organic matter (SOM) gradient

along the length of the field which must be taken into account for soil water content considerations. More specifically there is an increase of SOM from blocks 1-2 to block 5 (Appendix I).

In 2022, the cash crop was maize (*Zea mays*), which was sown on April 14th, 2022 in 7 parallel rows following east–west row direction. The maize plants emerged on May 13th and were harvested on August 25th, 2022 after a 135-day life span. To eliminate interference from nutritional stress and weeds, fertilizers, and herbicides were applied according to the local cultivation practices. As part of the weed management strategy and cover crop termination, ploughing of cover crop biomass was performed before maize sowing. The availability of water for plants is described by wilting point and field capacity. For this textural classification, wilting point and field capacity were obtained from the water retention curve (not displayed) and reported to be around 3 and 13%, respectively. Irrigation was not provided and, in the summer of 2022, the study area had several rainfalls which occurred before June 27th, which is the first day of data collection. In August, precipitation events were scarce and only two light rain occurrences were documented two days before the last data collection (Appendix II).

2.2 Field and UAV Data Collection

2.2.1 Field data

During the growing season, 3 field campaigns and UAV flights took place on the days reported in Table 1. The choice of dates was dictated by the need to analyse maize throughout the growing season. These field campaigns correspond to the V12 stage considered to be the active growth and leaves/cob development stage, the R2 stage in which the kernel develops, and the R5 stage which is the final critical production stage of physiological maturity (grain filling). Biomass measurements occurred 1-5 days before or after the UAV flights. Biomass measurements include dried leaves weight (DLW) and water content in the leaves expressed as a percentage (PWC). Besides leaf measurements, samples of maize cob were collected (dried fruit weight or DFW) and used as a measure of maize production.

In each plot, 3 sampling sites were selected for data collection of biomass weights and moisture (leaves and stem) and the average values of these three readings were used to represent the sampling plot. Analysis of the samples was conducted in the laboratories of Wageningen University, on the same day of biomass collection. Weights before and after sample drying at 105°C for 24 h were taken and moisture content in the plants' components were calculated using the following formula (1):

$$\text{Moisture content (\%)} = (W2 - W3) / (W2-W1) \times 100 \quad (1)$$

where, W1 corresponds to the weight of the container with the lid, while W2 and W3 are the weights of the container with lid plus sample before and after drying, respectively.

Additionally, the soil water content (SMC, in Siemens) in the centre of each plot was measured every fifteen minutes using the traditional gravimetric method with TMS-4 dataloggers (Wild J., 2019). The gravimetric measurements are later converted into volumetric water content. The deployed sensor was located in the ground at the effective rooting depth (0–12 cm).

Maize is expected not to be affected by rapid changes in external conditions, such as water in the soil, due to its isohydric nature (Ihuoma and Madramootoo, 2017). Because of this, an average of the SMC readings before and during the flight on the day of the UAV campaign was considered and used in the analysis (for timing refer to Table 1).

Table 1 Summary of UAV, ground measurements and captured growth stages of maize (from vegetative phases to physiological maturity) according to Nleya et al. (2019).

| | Growth stage | Stage description | Field data | | UAV drone flight |
			Biomass	SMC	Thermal and multispectral
	Vegetative V12	Tassel develops rapidly. Lateral shoots and cob development.	June 22nd	June 27th – 00:00-12.45	June 27th - 12:30-12:50
	Reproductive R2	Kernel development. Silking stage	August 10th	August 9th – 00:00-16:30	August 9th - 16:08-16:36
	Reproductive R5	Physiological maturity and drying of kernels. End of mass gain	August 22nd	August 23rd – 00:00-17:45	August 23rd - 17:22-17:50

2.2.2 UAV Thermal and RGB Imaging Systems

In this study, a quad-rotor UAV remote sensing system (DJI Matrice 210 (RTK)) equipped with a FLIR Tau 2 thermal camera (FLIR Systems, Wilsonville, OR, USA) and an Hiphen Airphen multispectral camera (Hiphen, Agricultural Imaging Solutions, Avignon, France) was used. The main technical parameters are shown in Table 2. Flight planning was conducted with DJIFlightPlanner software (DJI, 2022), which allows the user to generate a route of waypoints from the desired take-off point.

Table 2 Main parameters of UAV thermal and RGB image acquisition system.

Camera	Parameter	Value
UAV thermal image acquisition system (FLIR Tau 2 19 mm)	Imager resolution	640 x 512 pixels
	Lens focal length	19 mm
	Spectral bands	7.5–13.5 μm
	Lens field of view	32°x 26°
	Accuracy	-25 to +100°C
	Thermal sensitivity (NETD)	<50mK
	Weight (camera + lens)	< 70 g
Multispectral image acquisition system (Hiphen Airphen, 6 bands)	Imager resolution	1280 x 960 pixels
	Band range	6 spectral bands among [450/530/570/675/710/730/750/850 nm] (FWHM=10nm)
	Lens field of view	8mm - 33°x26° / 4.2mm - 60°x46°
	Image format	TIFF

2.2.3 Acquisition and Pre-treatment of UAV Thermal and RGB Images

The accuracy of temperature measurements is influenced by ambient environmental conditions such as relative humidity, air temperature, the temperature of the surrounding objects, and the distance between the FLIR Tau 2 camera and the target. In this case, the meteorological effect was minimized by flying in absence of rain, snow, and dust (Messina and Modica, 2020). However, the passage of clouds could not be avoided during certain flights (June 27th and August 23rd), and because of technical issues, all flights except the first were accomplished late in the afternoon, therefore the shadowing effect is always present to a certain degree (Table 1). A trade-off with the battery duration was obtained by flying at an altitude of 20 m, which allowed to cover the area of interest in 20 minutes with 80% front and side overlap between images. Before every flight, a 20 minutes stabilization on the ground was adopted for reducing the systematic error and camera digital number (DN) shift due to wind and ambient temperature (Kelly et al., 2019). Additionally, the camera was set to perform non-uniformity correction every 20 seconds throughout the flight to account for possible detector drifts. Besides the thermal data acquired with FLIR Tau 2 facing downward vertically, multispectral images were captured with Hiphen Airphen provided of 6 bands (specifics in Table 2). The colour balancing feature with Agisoft Metashape (AGISOFT, 2023) that aims to normalize pixel values based on a comparison of common areas was used at the moment of orthomosaic creation. Colour calibration was done using the tie points as the source data. After images were acquired, mosaic processing was performed using Agisoft Metashape software. Thermal and RGB orthomosaics were geo-referenced using from five to seven ground control points whose coordinates were measured using an RTK differential GNSS device (Topcon HIPER V) with precision within 1 cm.

2.3 Canopy Temperature Extraction Method

For this study, two methods for extraction of vegetation pixels were investigated, based on thresholding of the NDVI and Otsu algorithm. For NDVI calculation (2), multispectral images were used and after several trials

with different thresholds for vegetation, an arbitrary value set to 0.45 was adopted (Nandibewoor et al., 2015).

$$NDVI = (NIR - RED) / (NIR + RED) \quad (2)$$

For the Otsu algorithm, RGB images were further processed following the steps shown in Figure 2. Following this method, georeferenced optical image orthomosaics were converted into greyscale imagery using equation (3). The resulting single-band orthomosaic underwent a back- and foreground separation based on the frequency distribution of pixels. Otsu algorithm segments the image making the variance on each of the classes of a greyscale image minimal (Otsu, 1979).

$$GREYSCALE\ INTENSITY = 0.2989 * RED + 0.587 * GREEN + 0.1140 * BLUE \quad (3)$$
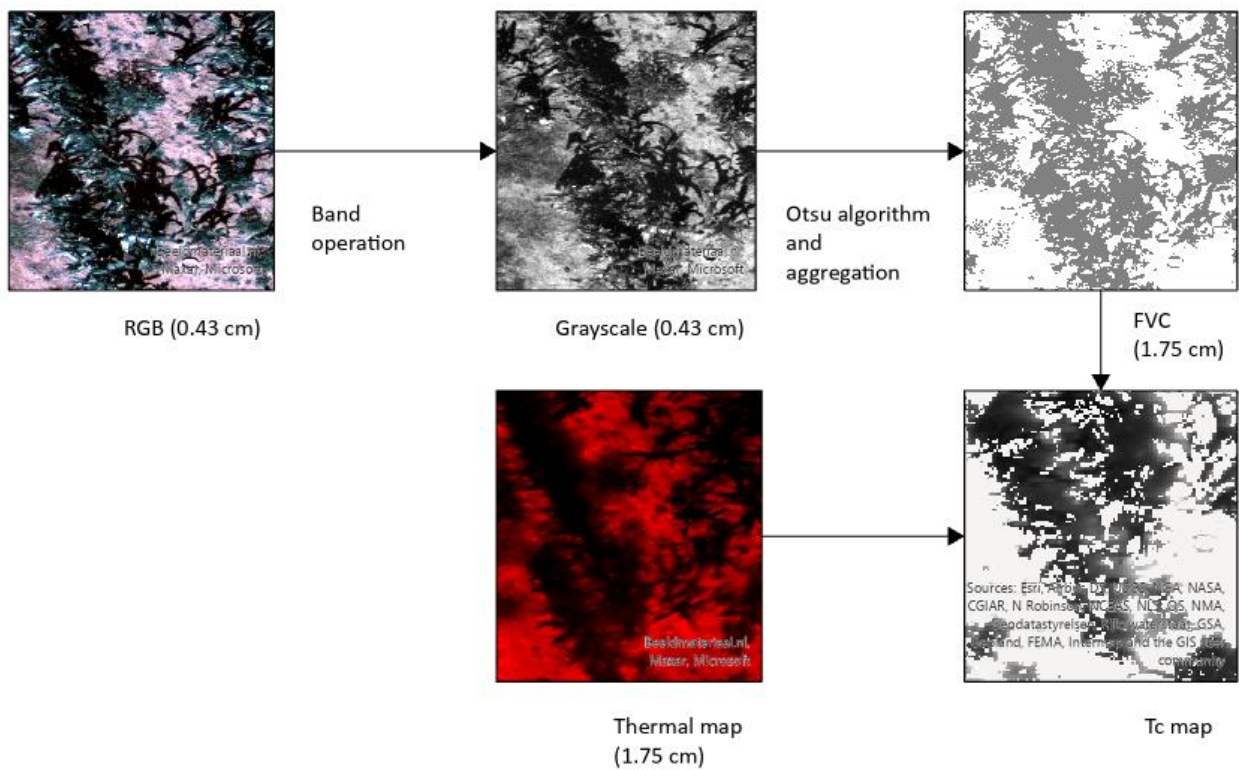

Figure 2 The main steps of the co-registration approach Otsu method proposed in this study using both unmanned aerial vehicle (UAV) thermal and red–green–blue (RGB) remote sensing imagery. FVC (fractional vegetation cover) and greyscale were derived from optical image.

The segmented orthomosaic was then used to mask the georeferenced thermal image orthomosaic for having a resulting T_c map, after resampling from 0.43 to 1.75 cm by using the nearest-neighbour interpolation algorithm (Figure 2). The entire process of the RGRI-Otsu method was implemented in R programming language (RStudio, 2022) and ArcGIS Pro desktop (Redlands, 2022). Similarly, the resulting NDVI-based mask from the same day was overlaid with the thermal data. The resultant T_c maps for each of the three UAV flights were then subjected to an accuracy assessment. Accuracy assessment was done by comparing the results of the two adopted methods to the RGB orthomosaics. With random sampling, 500 thermal pixels were selected and assessed based on the visual interpretation of the RGB image. Paired pixels were counted as True Positive, predicted canopy pixels in the T_c map that were not paired with vegetation in RGB as False Positive,

and canopy in RGB without a pair in T_c were assigned False Negative. Based on this information, the producer's accuracy for soil is calculated as the number of soil pixels in RGB classified accurately as such divided by the total number of reference sites for that class. As a further step for ensuring T_c was reflecting only vegetation, median T_c was used in the following analysis.

2.4 Statistical Analysis

2.4.1 Multilinear regression and correlation

After the accuracy assessment, the method with the highest producer's accuracy for soil pixels for each day was selected and used for statistical analysis. The relationships between ground measurements and maize median T_c for each field campaign-UAV flight were explored using multilinear regression. Specifically, linear regression models were used with the coefficient of determination (R^2) and *p-value* calculated for comparisons. The regressions were implemented by using R programming language and lm() function (Fox J., 2019). DFW is not considered in multilinear regression since other components of maize plants such as maize fruit and stems are not determinant for plant transpiration, therefore DFW is assumed to be a variable with no effect on T_c.

2.4.2 Analysis of Variance and Post-Hoc Test

Two-way analysis of variance (ANOVA) was used to investigate the effect of varying cover crops and the effect of SOM gradient over the field on the median T_c. ANOVA was applied using R programming language. Tukey's Honestly Significant Difference (Tukey's HSD) post-hoc test was used to perform pair-wise comparisons between cover crop treatments. Homoscedasticity and normality were checked with Levene and Shapiro test, respectively. Finally, the *p-value* and the coefficient of determination (R^2) were obtained to explore the significant relationships. During this study, a level of 5% was considered significant (*p-value* < 0.05).

3 Results

## 3.1 Removal of Soil Background Pixels in the Crop Research Plots

On the 9th of August, NDVI selection results in an accurate classification of vegetation (0.98) at the expense of lower producer's accuracy for soil compared to Otsu (0.55 and 0.87, respectively) (Table 3). On the same day, the Otsu method identified more soil pixels correctly than NDVI and have a comparable high producer's accuracy for vegetation (0.86) (Table 3). Therefore, the T_c map derived from Otsu on the 9th of August offers a clearer picture of maize temperature, which is less contaminated by soil readings. Whilst the Otsu method performed at its best on the 9th of August 2022 (331 soil pixels correctly classified), its performance declined to 57 pixels on the 23rd of August 2022 (Table 3). Unlike Otsu separation, the NDVI method with a fixed 0.45 threshold results in an overall low but stable performance on the two dates (85 and 82 soil pixels correctly classified), which makes it a better option for extracting T_c on 23rd August 2022. Furthermore, the NDVI method performed better on the 27th of June. In this case, the NDVI producer's accuracy for soil is 0.96 against 0.63 reported for the Otsu method (Table 3).

Table 3 Results of accuracy assessments performed on 500 random points.

Dates	Class	Otsu method		NDVI method	
		Producer's accuracy	Pixels correctly classified	Producer's accuracy	Pixels correctly classified
27th of June	Vegetation	0.80	231	0.83	238
	Soil	0.63	135	**0.96**	207
9th of August	Vegetation	0.86	301	0.98	342
	Soil	**0.87**	134	0.55	85
23rd of August	Vegetation	0.87	331	0.89	341
	Soil	0.47	57	**0.67**	82

Figure 3 shows the frequency distributions of greyscale pixels (A) and thermal pixels (B and C). A greyscale image is the monochromatic representation of RGB in which only pixel intensity information counts. The greyscale image is computed before the Otsu algorithm and the pixel pattern distribution dictates the success of Otsu separation. The thermal pixels are displayed before (B) and after (C) use of Otsu and NDVI methods on data acquired on the three days with UAV flight campaigns. From the comparison of Figure 3 B-C and Figure 4 B on the 9th of August, the two methods show potential for removing the pixels with higher temperature values corresponding to soil or other non-vegetative components present in the field. Both methods give a skewed right distribution of pixels representing maize canopy temperature. However, they differ in the frequency of pixels that are classified as vegetation, with the NDVI method considering more pixels as a canopy on the 9th of August. Unlike the 9th of August, on 23rd August 2022, the overall temperature distribution within field plots, which has its maximum value at 41.6°C, does not present the two typical peaks associated with left- and right-shifted vegetation and soil temperatures. The resulting T_c maps show the same range of temperatures of the overall field temperature and do not significantly differ from each other. Similar patterns to (B) can be seen in the pixels frequency distribution of the greyscale images (A) for the 9th and 23rd of August. However, this does not apply on the 27th of June, as a different distribution is found for greyscale

and thermal pixels. In (A), unimodality is reported, while in (B) thermal pixels are spread over a narrow and low-temperature range (2-17° C). The thermal pixel distribution in this range has three peaks and the highest peak is at around 13° C. The distribution is maintained after the application of NDVI and Otsu separations.
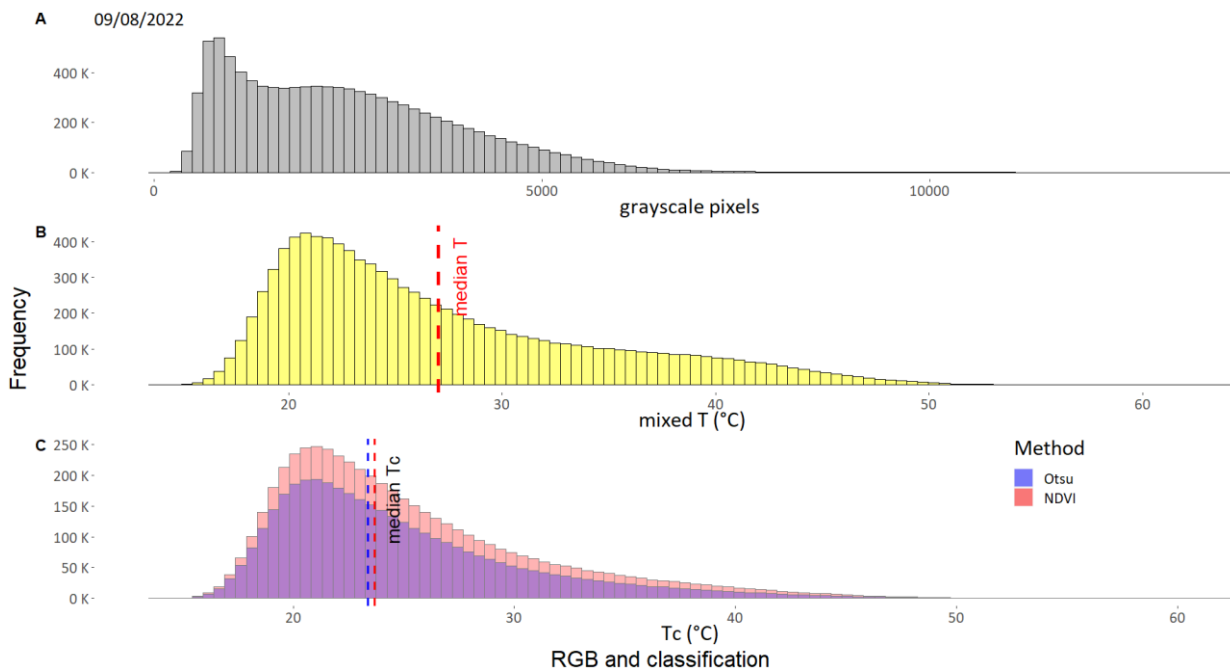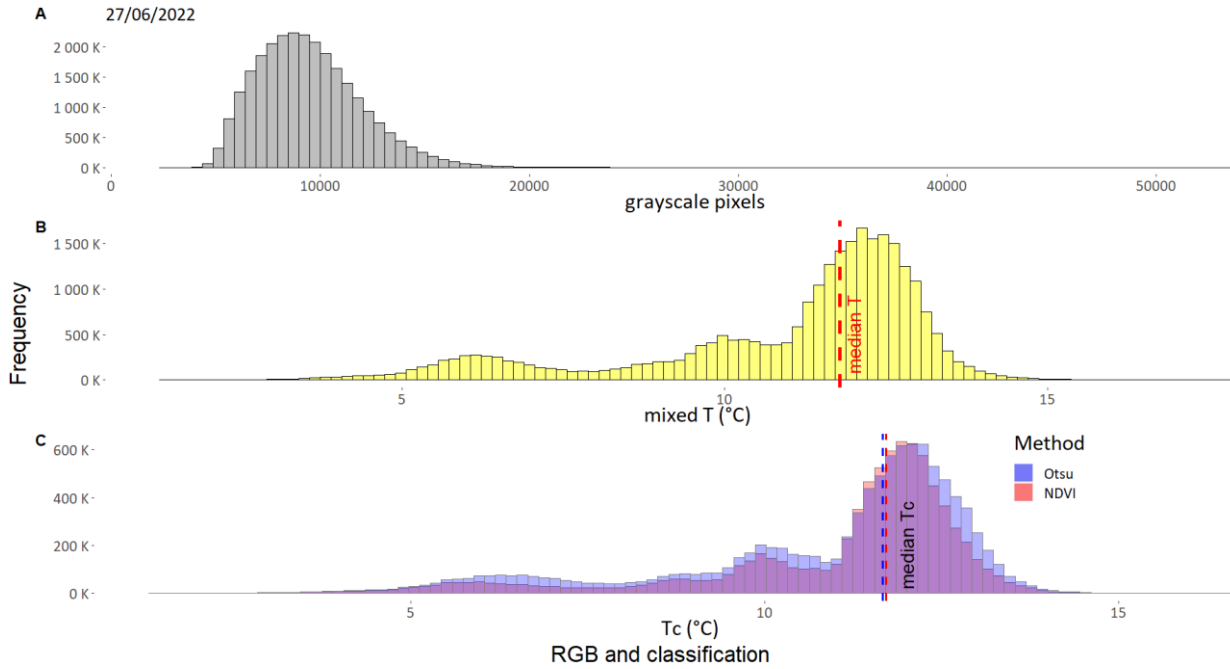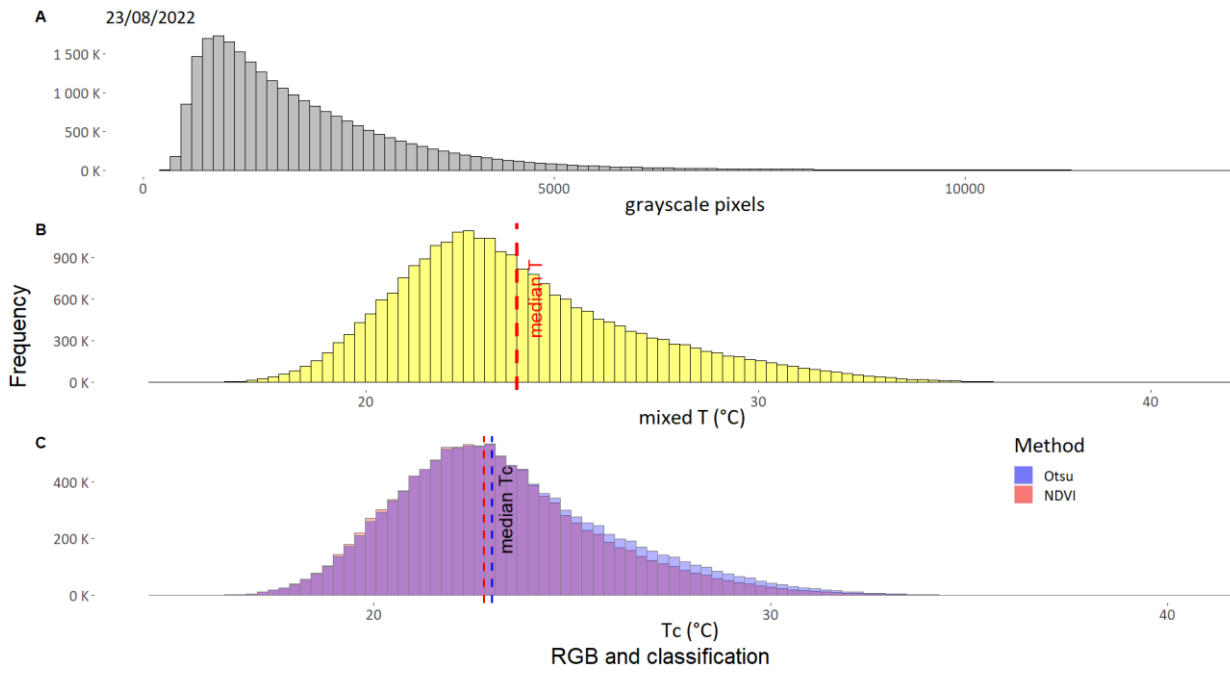
Figure 3 Greyscale pixels distribution (A) and pixel-based temperatures before soil removal (B) and after (C). Median values for mixed temperature and T_c in B and C respectively are shown as dashed line.

A

B

C

Figure 4 Zoomed RGB and NDVI-Otsu segmentation. The chosen selected method on each day is <u>underlined</u> (vegetation in green, soil in pink-brown. Block 3 "OR" is shown).

3.2 Relationship between UAV-based and ground-based measurements

From the results of correlation analysis which are shown in Figure 5, T_c negatively correlates with SMC and both biomass measurements (PWC and DLW) on all investigated days. However, the strength of this correlation varied. On the 9th of August, the relationship between T_c and PWC is the strongest (correlation coefficient=-0.67 ***), followed by DLW in the second place and SMC (correlation coefficient=-0.58 *** and -0.30 ***, respectively). These relations become overall weaker on the 23rd of August and the order changed. Similarly to the 9th of August, on the 23rd, a strong correlation between T_c and PWC is also highlighted (correlation coefficient=-0.40 ***). However, on this date SMC is reported to influence T_c more than DLW (correlation coefficient=-0.35 *** and -0.19 **, respectively). Furthermore, the correlation plot shows a positive relation between SMC and PWC which was taken one day after, on the 10th of August (Figure 5 A). On the 23rd of August, the relation subsides and is not significant (Figure 5 B).

A - Reproductive phase R2 - 9/08/2022
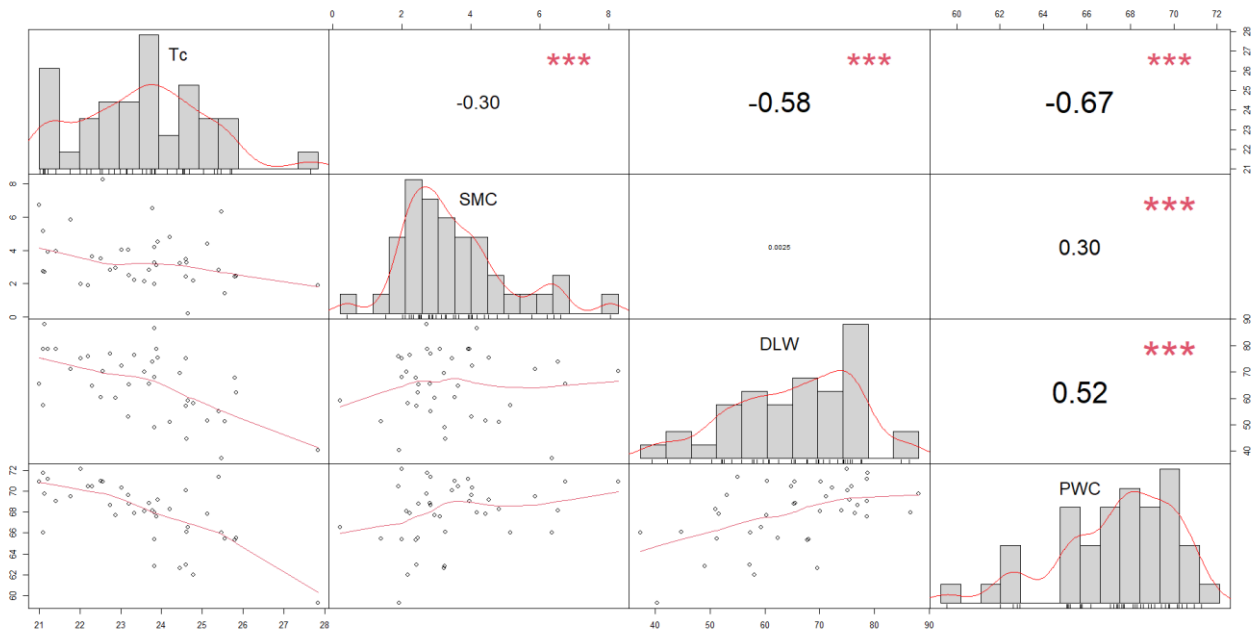
B - Reproductive phase R5 - 23/08/2022
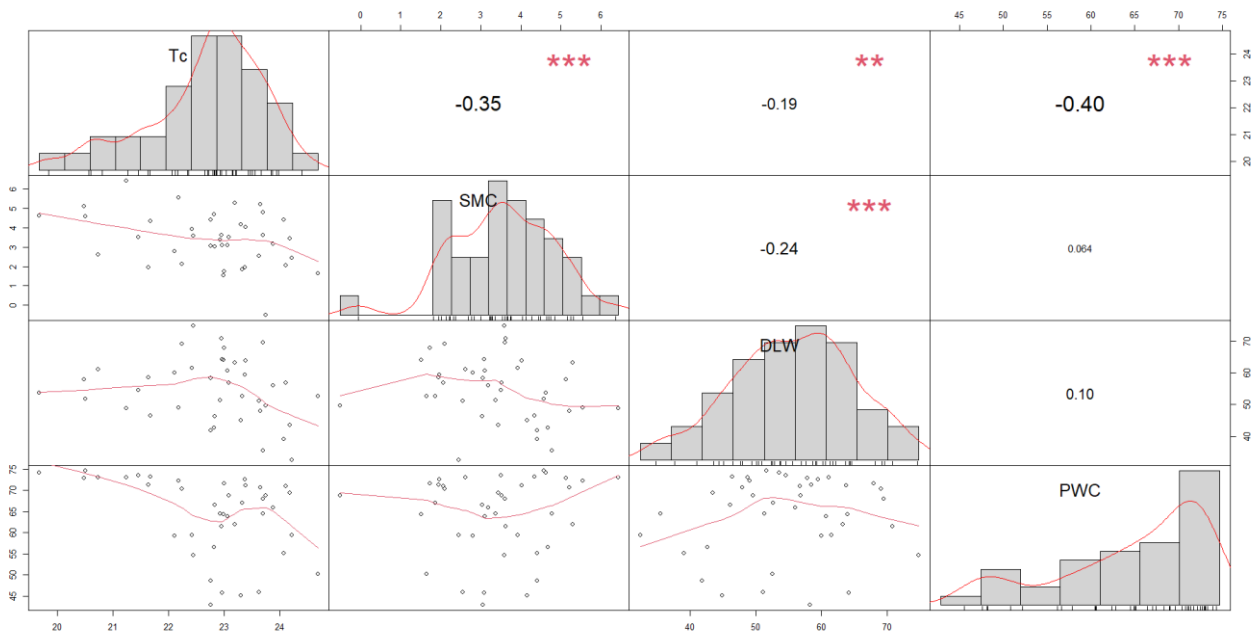
*Figure 5 A and B correlation plots display the correlations on the 9th and 23rd of August, respectively. On the diagonal, the distribution of each variable is shown. Below the diagonal and above it, scatterplot with fitted lines and correlation with significance level are reported, respectively. p-values of 0.001, 0.01, 0.05, 0.1, 1 correspond to "***", "**", "*", ".", " ".*

On the 27th of June, linear regression and correlation analysis were conducted twice, with all the blocks and with the exclusion of blocks 2 and 4, which from a visual inspection present non-uniform distribution of temperature (Figure 6). When blocks 2 and 4 are considered, the correlations with T_c are weak and insignificant either between biomass measurements which were taken five days before and the SMC sampled on the day of the flight (not displayed). Nonetheless, when the readings from the two blocks are excluded from analysis, PWC and DLW become able to influence T_c to a certain degree (correlation

21

coefficient=-0.49 * and -0.45 *, respectively) (Appendix III). However, in this scenario, there is no significant correlation between SMC and T_c.
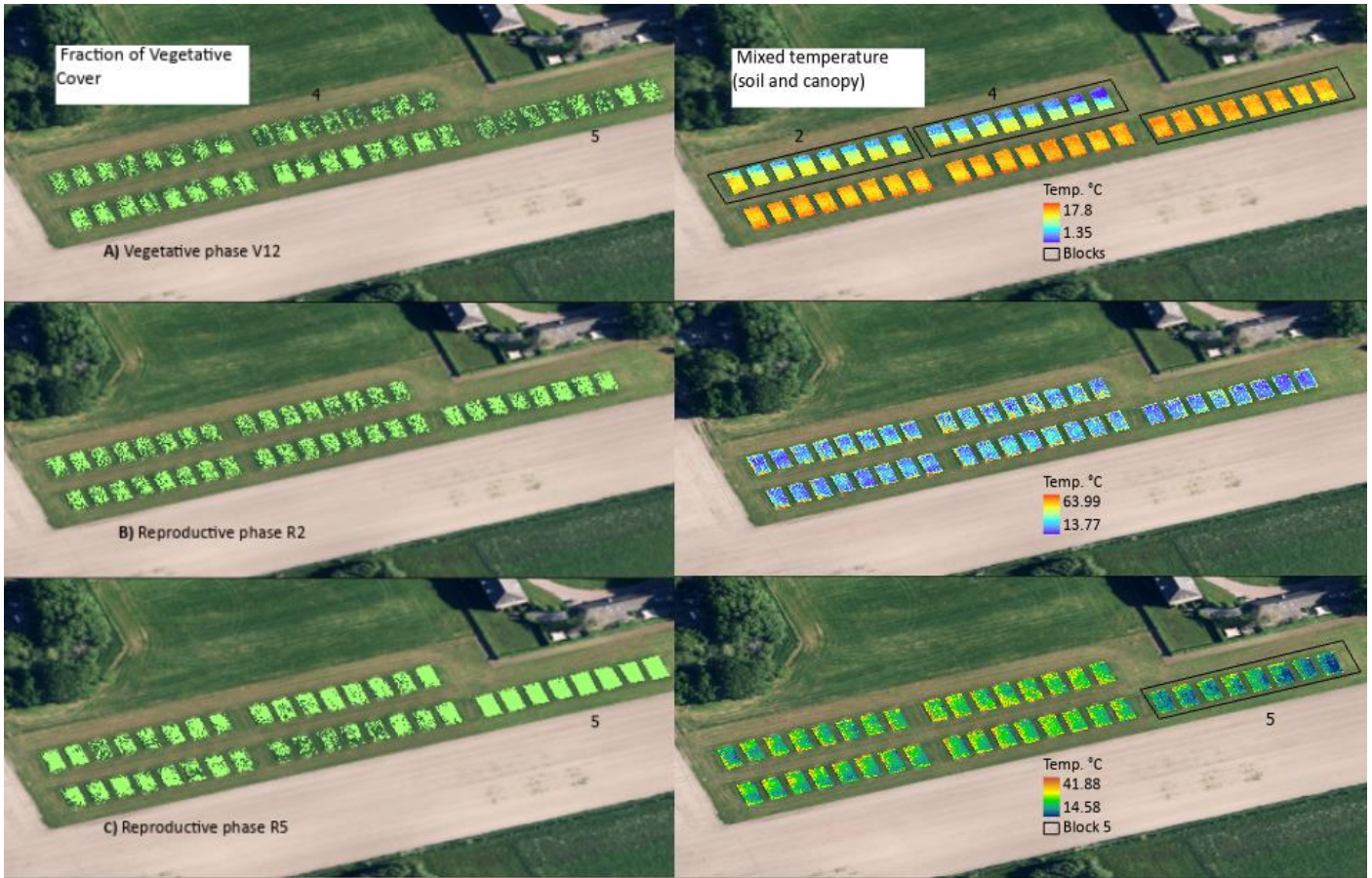
Figure 6 Canopy cover in green after application of the selected soil-pixel exclusion method (left) and thermal orthomosaic (right).

Results from linear regression are presented in Table 4, which illustrates the relationships between selected T_c-predictor variables and median T_c. Overall, on the 9th of August, there was a significant negative correlation between T_c and PWC, DLW, and SMC ($p < 0.001$) with an adjusted R^2 of 0.50 (Table 4). When the relationships are taken individually, the largest R^2 of 0.44 is found for median T_c and PWC, while R^2 of 0.33 and 0.09 for DLW and SMC, respectively (results not displayed). Interestingly, 4 out of 8 measurements from block 3 present lower PWC than the rest of the samples for the 9th of August. In particular, maize after fallow treatment has less than 60% PWC (Figure 7 B). For the range of PWC within which most of the measurements are, 4 out of 8 samples from block 5 have the lowest T_c reported for the 9th of August. Similarly to the 9th of August, a significant negative correlation between T_c and PWC, DLW, and SMC is reported for the 23rd of August, which however results in R^2 of 0.26 ($p < 0.001$). In the relationship between PWC, SMC, and DLW with T_c, changes of PWC show to be slightly better linearly related with variations of maize temperature (Figure 7 C). Also in this case, block 5 presents the lowest T_c reported for that day (Figure 7 C). On the 27th of June, PWC, SMC, and DLW do not impact the T_c, unless blocks 2 and 4 are excluded from the analysis (Table 4). After this step is performed, PWC and DLW become relevant in influencing T_c (R^2=0.44, $p < 0.001$) and PWC has the strongest influence (Figure 7 A). From one day to the other, a progressive shift of the PWC range to lower values is documented. However, for some measurements, such as from block 5, the PWC on the 23rd of August continues to be similar to the initial values measured on the 27th of June (Figure 7 A, B, C).

Dates	R^2 and p
27th of June	0.03 / 0.44 ***
	(with and without block 2 and 4)
9th of August	0.50 ***
23rd of August	0.26 ***
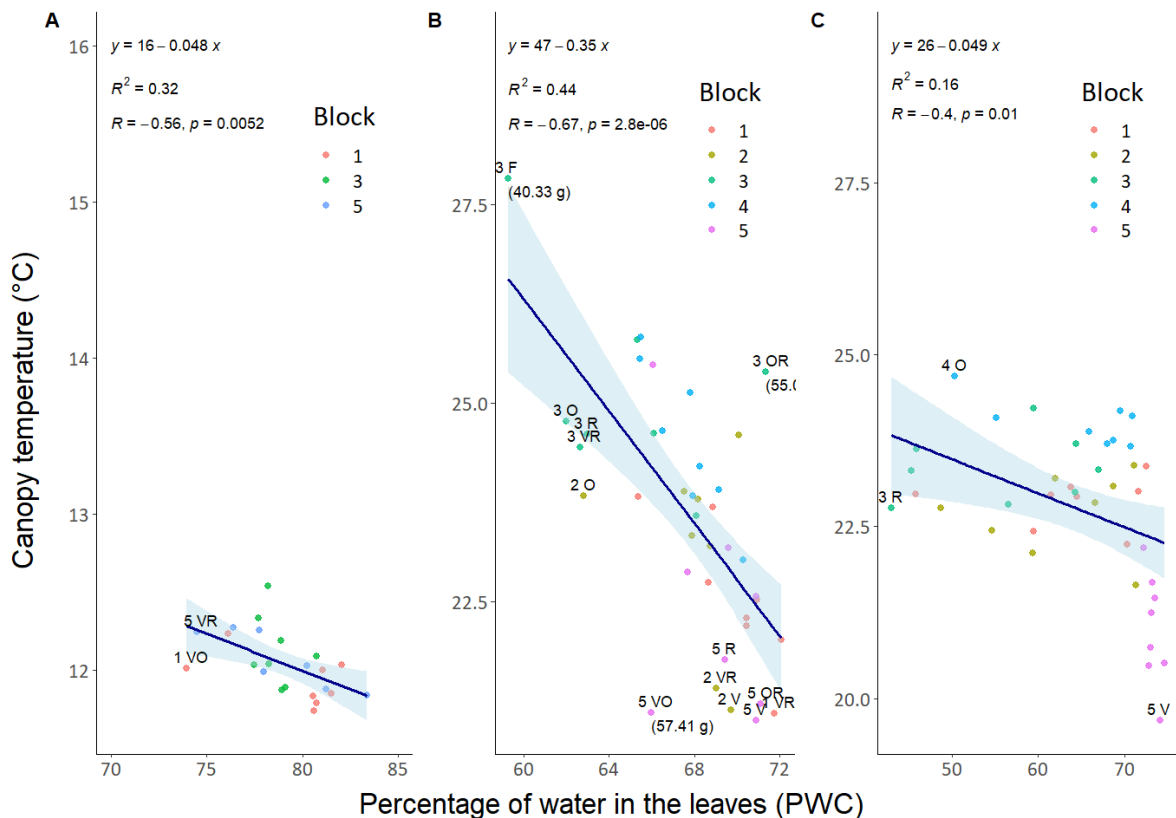
*Figure 7 Pearson's correlation between median T_c and PWC for June 27th, August 9th and 23rd respectively (A, B and C). Block subdivision is highlighted in colours and treatment types are specified with their labels. p value: 0 '***' 0.001 '**' 0.01 '*' 0.05 '.' 0.1 ' ' 1.*

3.3 Cover crop influence on the canopy temperature – soil water content relationship

Results from two-way Anova confirm an influence of blocks for all factors on the 9th and 23rd of August (not displayed). For the two dates, treatment effect given by cover crops is generally present for all factors, except for SMC (Figure 8 and 9). In addition, on August 23rd, cover crop use does not show to influence median T_c (Figure 9). On the 27th of June, treatments influence SMC (Appendix IV) while block presence is reported to have a significant impact only on T_c and DLW (not displayed). Differences between blocks can be also visually assessed in Figure 6. On the 27th of June, block 5 and 4 present canopy gaps and larger areas of exposed soil (visible in Figure 6, on the top left), while the thermal map shows a gradient of lower to higher temperatures within blocks 2 and 4 moving from field border to inner aisle (Figure 6, on the top right). On the 23rd of August,

the vegetation in most blocks is yellow (Appendix V) with the exception of block 5 where green vegetation cover is present and accompanied by lower T_c (Figure 6, on bottom left and right).

On the 27th of June, SMC is measured to be around field capacity values (10-13%) (Appendix II), and a small but significant difference is found between treatments (Appendix IV). Vetch-oat ("VO") results in more soil water in comparison to vetch-oat-radish ("VOR") and radish alone ("R"). On the 9th and 23rd of August, SMC readings suggest that the field is close to wilting capacity (Appendix II) and as stated beforehand SMC values do not differ significantly between the plots previously cultivated with different cover crops (Figure 8 and 9). However, a pattern is found between T_c, PWC, DLW, and DFW for certain crops. For example, on the 9th of August for control (fallow "F"), a higher maize T_c than vetch ("V") and vetch-radish ("VR") is associated with reduced dried leaves and fruit weight in comparison to vetch-radish (Figure 8 C, D and E) (significant difference ($p < 0.05$) between treatments is indicated with the letter "a" and "b"). At the same time, a lower T_c for maize grown after vetch relates with a significantly higher PWC than that found in maize after oat ("O") (Figure 8 A and B). The latter one, when mixed with radish, does not differ from vetch alone in terms of PWC (Figure 8 A). A positive correlation between moisture in the leaves and DLW/DFW is found for oat-radish and oat, respectively (Figure 8 A, D, and E).

Figure 8 The distributions of leaves moisture, maize T_c, soil moisture content, dried leaves weight and dried fruit weight of maize after 8 cover crops treatment for the 9th of August. Lowercase letters indicate significant differences between treatments and a different letter indicate significant differences between treatments (p < 0.05).

On the 23rd of August, vetch and oat-radish maintain the significantly higher PWC found on the 9th of August, which is accompanied in this case by higher DFW for the oat-radish combination (Figure 9 A and E). As it was reported on the 9th, on the 23rd of August oat alone was associated with lower PWC and DFW in maize. For

the first time on the 23rd of August, the combination of the 3 cover crops ("VOR") led to a significant increase in PWC and DFW (Figure 9 A and E).
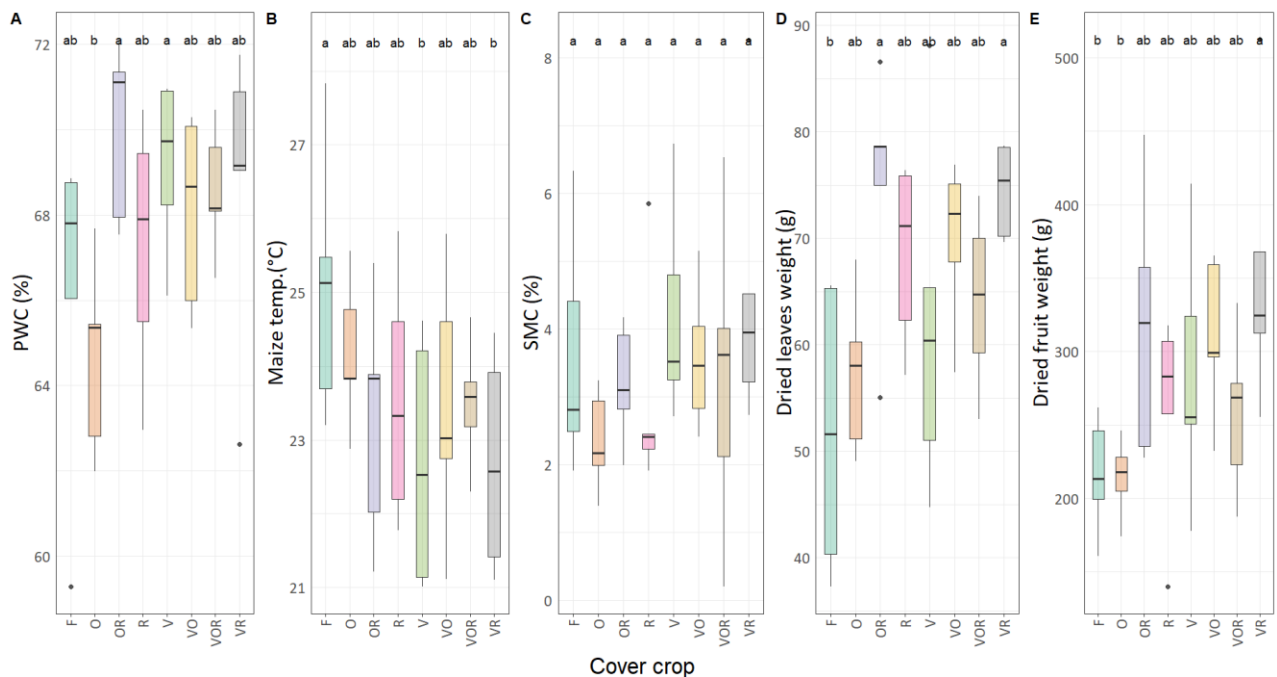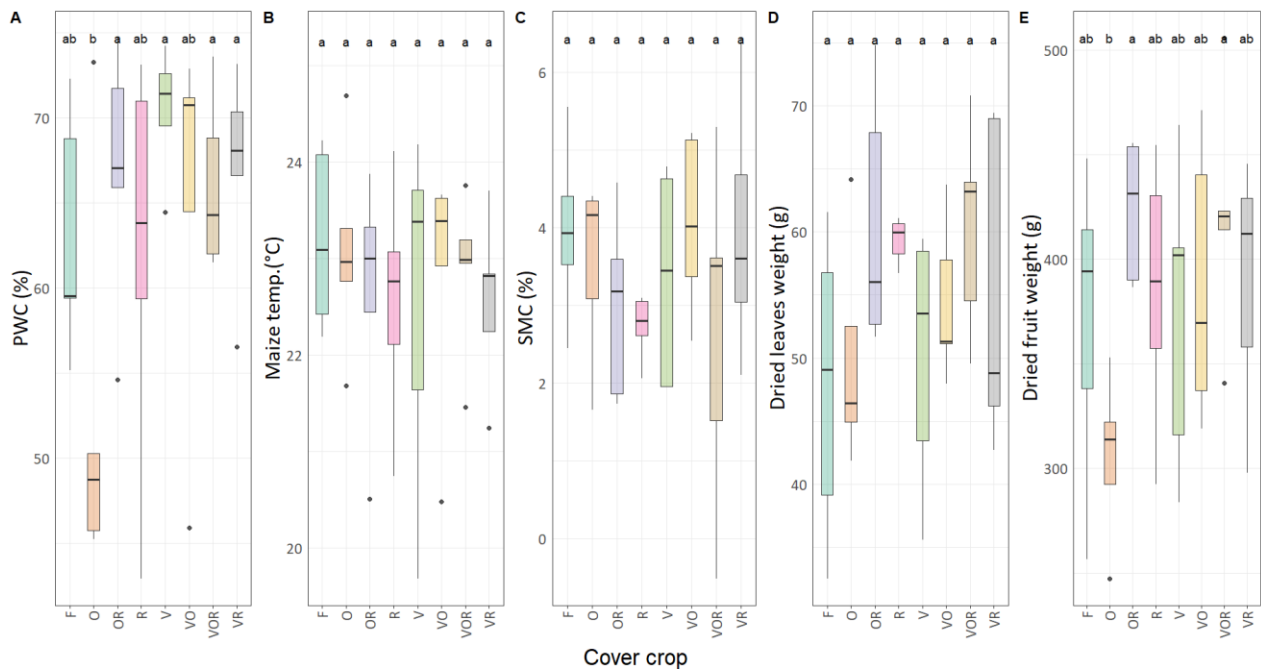

Figure 9 The distributions of leaves moisture, maize T_c, soil moisture content, dried leaves weight and dried fruit weight of maize after 8 cover crops treatment for the 23rd of August. Lowercase letters indicate significant differences between treatments and a different letter indicate significant differences between treatments (p < 0.05).

4 Discussion

4.1 Soil pixels removal - NDVI and Otsu algorithm accuracy for soil exclusion and vegetation selection

In this paragraph, the effectiveness of the Otsu algorithm in excluding soil pixels is examined by analysing how different factors, such as maize size and colour, affect its performance at various stages of maize growth. Subsequently, the accuracy of NDVI is discussed in relation to these findings.

In general, Otsu is frequently employed for image segmentation because of its straightforward algorithm and high level of automation. However, Otsu performs well in segmenting images with bimodal variance between classes, which may not always be present (Song et al., 2022). On August 9th, the bimodal variance was observed in the greyscale image obtained from RGB, allowing for the application of Otsu. In contrast, its absence on other dates hindered its effectiveness (Goh et al., 2018). Goh et al. (2018) also found that image parameters such as intensity level between vegetation class and background, vegetation size, vegetation position, and noise can impact the performance of Otsu thresholding. This was evident in the imagery from August 23rd, where vegetation intensity was very dim and close to background intensity (Appendix V), resulting in confusion between yellow leaves and bright soil. Additionally, the image was noisy and contained regions with different intensities, which may have affected the segmentation due to Otsu using the intensity of the entire image, potentially leading to local colour imbalances.

On the other hand, unlike on August 23rd, Otsu's accuracy on June 27th may have been limited by the inverted size of the foreground and background. In this case, the background represented by soil was predominant over maize as the crop was in the starting phase V12, which was especially noticeable in blocks 5 and 4 where vegetation growth appeared stunted and scarce (Figure 6, top left). Furthermore, sunlit leaves, which appeared brighter, were seemingly assigned to the background class, increasing the frequency of greyscale pixels for this class (Figure 3).

Although Otsu thresholding may not be effective in extracting soil at the beginning and end of maize growth, it performs reasonably well in detecting vegetation on the three dates. The producer's accuracy for vegetation, which ranges between 80% to 87%, remains high throughout the summer, including the early growth stages, as reported by García-Martínez et al. (2020). Similarly to this thesis, García-Martínez et al. (2020) found vegetation cover estimations with errors of less than 5% in the early stages of maize development. During the crop's growth, García-Martínez et al. (2020) observed that applying Otsu after using the Excess Green index (ExGI) resulted in errors ranging from 2.2% to 17.8% in estimating the vegetation cover fraction. In the case of a complex photo background with soil and weeds, Meyer and Camargo Neto (2008) reported an accuracy of approximately 50% for ExG and Otsu in detecting vegetation, while accuracy reached 88% in the case of a simple background with bare soil. Song et al. (2022) also found that the accuracy of ExGI plus Otsu was approximately 50%, which is substantially lower than the accuracy found in this study for all three days. García-Martínez et al. (2020), Meyer and Camargo Neto (2008), and Song et al. (2022) use the Excess Green index on which Otsu thresholding is applied, instead of the more common greyscale intensity image obtained from RGB. The ExGI index uses the contrast between the green, red, and blue portions of the spectrum to differentiate between vegetation and soil (Camargo Neto and Meyer, 2005; Vidović et al., 2016). Studies have shown that it performs better than other indices that rely only on RGB to distinguish vegetation (M. Woebbecke et al., 1995; Vidović et al., 2016). Specifically, the ExGI index is more effective in identifying weeds from non-vegetation backgrounds at a significance level of 0.05, albeit with higher computation requirements than other methods (M. Woebbecke et al., 1995). From comparison of results using ExGI (García-Martínez et al., 2020; Meyer and Camargo Neto, 2008; Song et al., 2022) and this thesis, the variant ExGI index is likely to have similar accuracy in estimating vegetation cover compared to Otsu applied to greyscale orthomosaics. This is true when weeds are not the focus of the analysis. However, if the study requires an accurate analysis of maize by excluding weeds along the plot borders, the ExGI index may be more appropriate than greyscale intensity.

Despite the high accuracy of Otsu on greyscale in selecting vegetation, NDVI results in even higher accuracy, ranging between 83% to 98% for the three days. On June 27th, sunlit leaves tended to be misclassified as soil by Otsu algorithm, resulting in a reduced level of plant identification accuracy for Otsu compared to NDVI. For the other two days, shadows were present as the UAV campaigns were conducted in the afternoon. In the absence of complementary techniques like Hue Saturation Intensity, NDVI tends to classify more shaded pixels as vegetation (Cai et al., 2010) and darker green pixels with lower temperatures are considered as canopy in our ground truth.

Since the initial stages, both Otsu and NDVI exhibited effective performance in vegetation selection. However, on August 23rd, NDVI could have achieved improved vegetation detection if the threshold value was set lower than 0.45. This is because in the later stages, some vegetation turns yellow, and accurate classification requires lower threshold values for NDVI. Generally, the histogram representation of thermal pixels reflects the typical temperature differences between soil and vegetation (Jones and Sirault, 2014), suggesting that TIR data could be used to fine-tune the NDVI threshold. As a recommendation for future research, incorporating initial temperature representation could optimize the separation process.

Additionally, incorporating thermographic information after applying the selected methods could provide an overview of the effectiveness of the separation process.

4.2 Relationships between ground measurements and thermal maps on field level

As hypothesized, this study shows that ground measurements of crop water stress are related to T_c. Correlation analysis results reported in Figure 5 indicate that on the 9th and 23rd of August, T_c negatively correlated with SMC, PWC, and DLW, suggesting that lower soil water content increases T_c through stomata closure. Similar effects were observed with the presence of water in the leaves (PWC) and the addition of vegetative layers represented by DLW. In the latter case, the total transpiration of a maize plant results from the sum of transpiration occurring in each leaf, indicating an additive effect. The choice to use DLW instead of the fresh weight of the leaves is because PWC already accounts for water content, and a measure of leaf weight alone or growth was needed. Acorsi and Gimenez (2021) used fresh biomass along with grain yield. Pearson's correlation analysis between these plant variables and T_c showed negative correlation values of 0.56 and 0.45, respectively, which are similar to values reported in previous studies on maize by Zia-Khan et al. (2012). In contrast, on the 27th of June, the correlations between biomass variables and T_c were weak and insignificant (correlation coefficient below 0.1) due to the passage of a cloud, which rendered 16 of 40 measurements unusable. The deviation of several point measurements in a small dataset may cause a divergence from the true relationship, which may not be observed for this reason. However, when diverging readings from blocks 2 and 4 were removed from the analysis (Table 4 and Figure 7), variations in PWC and DLW became significantly linearly related to T_c also on this day. The relationships may not be strong due to the 5 days between ground measurements and the UAV campaign. However, due to the isohydric nature of maize, it is expected that PWC may not have changed considerably within the five days. Maize maintains a stable leaf water status over a wide range of evaporative demands or soil water supplies (Ihuoma and Madramootoo, 2017; Tardieu and Simonneau, 1998), and therefore, a sudden change in soil water is not reflected in fast water uptake. In the opposite situation, maize steadily maintains leaf water content to a certain extent, as reported in this case. Regarding the combination of DLW-T_c on the 27th of June, the significant negative relationship found can be attributed to the voluminous and highly transpiring biomass that is typical of the V12 stage of maize growth (Nleya et al., 2019). However, substantial changes may have occurred between the days of biomass sampling and thermal data collection, which could impact the strength of the relationship. Therefore, the relationship between DLW and T_c could have been stronger if DLW measurements were taken on the same day as the UAV flight.

4.2.1   Soil water content-T_c

Among the relationship found, correlation analysis confirms a weak negative correlation between T_c and SMC on the 9th of August, which becomes stronger on the 23rd of August, as shown in Figure 5. On the 23rd of August, it is possible that DLW did not increase any longer, and the current biomass could not be highly transpiring, resulting in a lower impact of PWC on T_c. At this point of maize growth, SMC could not be obscured anymore and play a role in T_c changes. However, SMC still explains little of the observed T_c variations. The finding that SMC has little influence on T_c on the 9th and 23rd of August contradicts the results of a study by González-Dugo et al. (2006), in which the standard deviation of canopy temperature (sdT_c) was compared to CWSI, a well-known parameter used for irrigation scheduling and sdT_c was found to reflect SMC (R^2=0.77). Han et al. (2016) and González-Dugo et al. (2006) suggest that sdT_c could be used as an indicator of water stress due to its significant relationship with soil water deficit (SWD). However, in this thesis, median T_c was adopted instead of sdT_c to ensure that only vegetative pixels were used. Nevertheless, no evidence of sensitivity to water deficit was found for median T_c in this study, which contrasts with previous research on

sdT$_c$ as previously described and studies using mean T$_c$. For example, Acorsi and Gimenez (2021) found an R^2 of 0.42 between the mean T$_c$ and soil water status, which substantially increased to R^2=0.88 when soil physical attributes were introduced. According to the variable importance classification, T$_c$ ranked second among the 11 attributes included in the model for predicting water content (Acorsi and Gimenez, 2021; DeJonge et al., 2020). In Zhang et al. (2019), the use of different irrigation systems, resulting in a wider range of soil water contents, led to even higher R^2 values (between 0.40 and 0.53) for linear regression models between SMC at 0-0.2 m soil depth and T$_c$. In this thesis, there was no artificial irrigation, and the SMC observations were distributed over a narrow range of values, which may have unfavourably resulted in lower correlation values for the multilinear regression models.

Little effect of SMC on T$_c$ at later stages may also be due to variations in water uptake in the soil profile. Although maize typically relies on water from shallow soil depths taken up by lateral roots (Ahmed et al., 2015), de Lara et al. (2019) found that maize yield has a significant relationship with deeper SMC readings (90 to 150 cm) later during the growing season. Similar trends were detected by Hupet and Vanclooster (2002), whose research demonstrated that well-developed maize crops source water from deeper soil layers (50 to 100 cm). In our study, the SMC sensor is fixed at a shallow depth, and may not be able to detect changes in water demand by deeper roots occurring at later stages. The water that potentially influences T$_c$ on the 9th and 23rd of August may be located at deeper depths that are not considered by the SMC sensor. This fact may partially explain the absence of a significant relationship between SMC and T$_c$ on the 9th and the weaker significant relationship between T$_c$ and SMC on the 23rd of August. However, previous studies have indicated that around 40% of soil water extraction for maize still occurs in the first 25 cm depth, justifying the experimental setup (Zhang et al., 2019). As highlighted by Zhang et al. (2019), water uptake from superficial soil layers is seen in vegetative phases, and they reported significant correlations between T$_c$ and SMC measured at depths of 10, 20, and 30 cm, and no significant relationships at depths of 45, 60, and 90 cm. Additionally, the insignificant and weakly significant T$_c$-SMC relationship on the 9th and 23rd of August, respectively, may also be influenced by the fact that on both days, the observed SMC values were close to the wilting point. Wilting point was likely due to the dry season and the low water holding capacity of sandy soil. Consequently, there was little water in the soil for plant uptake.

Based on the results of this study, thermography using median T$_c$ cannot be considered a reliable proxy for SMC during the growing season of maize. However, recent research has shown the potential of RGB alone in assessing soil moisture. For instance, Lu et al. (2020) demonstrated that surface soil moisture (0-10 cm) in a mixed soil-vegetation setting can be estimated using the brightness of UAV visible images. While the application of RGB brightness is a novel concept, optical vegetation indices are a well-documented technique for SMC estimation. However, unlike thermography, vegetation indices capture past changes that occurred gradually in leaf pigments and do not provide real-time information. In their study, Wang et al. (2018) combined the advantages of vegetation indices and thermal information to estimate root-zone SMC in different soil-vegetation conditions, achieving accurate results (R^2=0.58–0.69 and RMSDs around 0.025 m$^3 \cdot$m^{-3}) using the "temperature-vegetation triangle approach".

4.2.2   Biomass-T$_c$

As crop growth progresses, there is a documented shift in the range of PWC towards lower values, from 70-85% on June 27th to 60-75% and 40-75% on the other two days, respectively. This suggests that maize leaves are maturing and approaching senescence. However, measurements from block 5 show that PWC on August 23rd remains similar to the initial values measured on June 27th, as mentioned in 0. This could be attributed to the later establishment of maize in block 5. Notably, at the time of harvest, NDVI of the entire block appears to have higher values, indicating good overall vegetation coverage and noticeable photosynthetic

activity, as evidenced by the lower T_c for that block (Figure 6, bottom right). Photosynthetic activity is closely related to SMC and PWC. In fact, increased soil water availability generally leads to increased stomatal conductance, allowing for transpiration and consequent cooling, as well as CO_2 assimilation for photosynthesis (Rossini et al., 2015). Results by Feng and Zhou (2018) indicate that maize PWC and SMC significantly affect the net photosynthetic rate in all developmental stages, which in turn is closely related to fruit yield and biomass growth (Rossini et al., 2015; Zhou et al., 2021), consistent with findings by Junior et al. (2021). Junior et al. (2021) reported that at 30% irrigation compared to 150% setting, only half of the stomatal conductance was observed, resulting in limited cooling of leaves. In this study, the SMC values found on August 9th and 23rd (maximum of 8%) correspond to the 30% irrigation condition in Junior et al. (2021), while the range of SMC values found on June 27th (around 10-14% SMC) can be compared to the 150% irrigation condition. Junior et al. (2021) also found that the highest net CO_2 assimilation rates, stomatal conductance, and transpiration rates were observed under the highest soil water availability conditions. Similarly to the limited water availability situation described by Junior et al. (2021), the reported T_c on August 9th and 23rd is likely a result of stomatal closure, indicating possible water stress in the crops. On August 23rd, the absence of bimodality in thermal pixels, as shown in Figure 3, suggests that the maize may no longer be actively transpiring or photosynthesizing, as its temperature is similar to that of the soil. Furthermore, the observed curled yellow leaves on August 23rd may also indicate dryness, as the PWC on that day does not strongly affect T_c. In contrast, on June 27th, when the soil is reported to be at field capacity, the canopy may still be actively transpiring and cooling down through stomata action. Furthermore, in V12 stage, high foliage leads to increased surface conductance, resulting in higher evapotranspiration, energy dissipation, and lower T_c, as reported by Ekinzog et al. (2022). Tall and dense canopies also attenuate radiation and reduce T_c, according to Westreenen et al. (2020). Through these mechanisms, biomass affects T_c in all stages, except during maturity when the DLW remains constant.

Besides the findings about SMC and leaves transpiration, Junior et al. (2021) indicated that the physiological indicators considered (stomatal conductance, transpiration, and net CO_2 assimilation rate), as well as NDVI, correlate with CWSI, suggesting that NDVI could be used as an alternative to assess maize water stress ($R^2 =$ 0.763; $p < 0.001$). Similarly, in Appendix VI, NDVI is shown to have a strong correlation with median T_c, indicating that it could be used not only to exclude soil pixels but also as a support for assessing maize water stress in conjunction with T_c. Recent methodologies have investigated integration of vegetation and temperature indices. Among these approaches, the temperature vegetation dryness index (TVDI), which is derived from land surface temperature (LST) and the NDVI, has gained widespread popularity to estimate soil moisture and vegetation water content (Wang et al., 2011).

In this study, we found that T_c can be used as a proxy for crop water status (PWC), but it is also influenced by DLW during growth. Incorporating NDVI as a normalization factor for T_c can offer advantages in assessing crop water stress, as it enables real-time monitoring of photosynthetic activity changes with higher temporal resolution compared to structural parameters such as DLW. Furthermore, previous reports by Wang et al. (2011) and Wang et al. (2018) have demonstrated NDVI's capability in estimating both SMC and PWC, indicating its potential to enhance the model when used with T_c.

Moreover, besides adding NDVI, the removal of SMC from the model may lead to an improvement, as it provides minimal or negligible information. Another rationale for excluding SMC is the interactive effect between PWC and SMC on August 9th (Figure 5 B). However, multicollinearity was not detected, as evidenced by VIF values close to 1 (Appendix VII).

4.3 Cover crop influence on the canopy temperature – soil water content relationship

4.3.1 Block effect

The role of soil organic matter (SOM) in influencing crop growth and water retention is explored in this paragraph through an analysis of its impact on various factors at different stages of maize growth, revealing the significance of SOM differences between blocks and their effect on crop establishment, development, and water retention. The prior knowledge about an existing SOM gradient in the field provides some explanation for our findings (Appendix I). The difference in SOM between blocks is found to be responsible for a significant difference for all the considered factors on all dates, except for SMC, DFW, and PWC on the 27th of June. In the beginning, on the 27th of June, maize may be facing equal conditions in all blocks, which start diverging with crop growth, kernel formation, and changing climatic factors due to SOM differences. In fact, on the 27th of June, the young thriving maize, which presents comparably high PWC in all blocks, is in the initial phase of cob development. Cob constitutes a fixed part of the DFW which is added to a variable kernel weight forming in the following phases. Besides, SMC in the starting phase ranges around higher values (field capacity) for all blocks and the SOM gradient effect in retaining water may not play a role. SOM's abilities to increase water retention in coarse sandy soils may start to be effective in more limited SMC conditions which are reported in August. According to Lal (2020), a small increase of SOM along the field leads to an increase in water holding capacity and stored water. The higher stored water in block 5 may be responsible for later maize establishment but at the same time may be the reason for healthier and transpiring vegetation observed in late August. As Tian et al. (2022) describe, with improved water content there is often lower soil temperature which leads to retarded germination rate and crop growth.

4.3.2 Treatment effect

(Expected) effect on SMC by treatments through soil structure and SOM addition mechanisms
The contribution of SOM within the field appears to have a greater impact on SMC compared to the expected SOM contribution from cover crop treatments. This is because variations in organic matter levels between blocks led to the observed effect on SMC, while treatments (except for "VO" on June 27th) did not show a significant influence. One documented mechanism by which cover crops are expected to contribute to changes in SMC is the addition of biomass, which is decomposed into organic compounds upon cover crop termination (Dabney et al., 2001; Koudahe et al., 2022). However, results from this study and Acharya et al. (2022) suggest that 6 and 5 years of repeated cover crop use may not have a significant impact on SOM storage.

Another mechanism by which cover crops could impact SMC is through the varying rooting system, which leads to different degrees of soil structure improvement (Koudahe et al., 2022). The use of cover crops in non-irrigated systems can be motivated by the potential for higher SMC after cover crop utilization, which is particularly desirable during the initial phase of cash crop growth. However, for reasons that are not identified, only on June 27th, the "VO" treatment contributed significantly higher SMC compared to "VOR" and "R". The treatment effect on SMC found on June 27th does not persist and remains limited to the initial phase.

The finding of no significant effect of cover crops on SMC or finding it only on one date suggests that there may be factors hindering this relationship, such as tillage. Araya et al. (2022) reported that soils under no-till and cover cropping systems improved soil structure in terms of pore size distribution, while changes in hydraulic conductivity under these systems led to increased infiltration rate and water retention. Tillage for terminating the cover crop and incorporating it may have compacted the soil, reducing pore size distribution and disturbing the soil structure improvement operated by cover crop roots. Soil structure is also conditioned by soil aggregates, and aggregates form and stabilize more easily in the presence of increasing levels of SOM

(Celik, 2005). Tillage may alter aggregate formation through the mechanical destruction of organic matter, which becomes more exposed to chemical and biological decomposition. Tian et al. (2022) indicate that no-tillage could be the solution for enhancing SOM, especially in sandy soil where soil aggregation is more difficult to obtain (Ayoubi et al., 2020). Restovich et al. (2022), in their no-till setup, demonstrated that the presence of SOM-enriched soil after 5-year cover crops, accompanied by stable soil aggregation due to a higher proportion of macropores and mesopores over 300 μm.

As previously mentioned, the higher SMC in the "VO" treatment during vegetative development on June 27th does not seem to bring any advantages over the other treatments. Even though higher water provision during the most demanding phase would be expected to favour maize growth in the following phases (de Lara et al., 2019), the "VO" treatment does not show any clear benefits in terms of maize growth and transpiration

Effect on biomass by treatments

The effect of some treatments on PWC and biomass growth can be seen on the 9th and 23rd of August. These effects are reflected in different maize T_c on the first day. Treatment "V" maintains a higher PWC over the two days which is accompanied by a significantly lower T_c on the 9th. When vetch is combined with radish to form "VR", there is an additional fertilizing effect seen as an increase of DLW and DFW, which however is not relevant for the final yield on the 23rd of August.

In general, legumes such as vetch result in a larger contribution of soil inorganic N compared to non-legume residues due to fast decomposition and nitrogen (N) release (Blanco-Canqui and Ruis, 2020; Koudahe et al., 2022; Piva et al., 2021). Furthermore, maize can benefit from additional N availability given by atmospheric N fixation during legume growth (Piva et al., 2021; Thapa et al., 2022). Elhakeem et al. (2023) showed how pure radish or in mixtures could increase N availability for the following crop by reducing N leaching up to 70% through a rapid uptake in autumn. Subsequently, residues from radish were reported to mineralize quickly, resulting in an increase of soil mineral N in spring at the time of maize sowing (70–110% more than fallow).

If "V" and "VR" show to contribute positively to maize, "O" is not helping the crop physiology and in addition, this treatment may have a more deteriorating effect on maize than fallow. Fallow, with an accompanying rise in T_c during growth, may result in delayed growth as observed on the 9th day. Despite this initial delay, the growth of maize after fallow is comparable to most of the treatments on the 23rd of August. Similarly, "O" treatment starts showing lower PWC associated with reduced DFW on the 9th, and this effect persists till the end, in accordance with Piva et al. (2021). Thapa et al. (2022) reported that oat, a grass cover crop with a high C:N ratio resulting in a lower mineralization rate, ultimately provided higher levels of SOC and total N compared to other cover crops. In this case, slower mineralization may be mismatched with maize growth and cash crop may not be benefitting from any of the positive effects of oat on the soil. Nitrogen and water are the major requirements for maize (Rafique, 2020), and oat treatment on the 9th and 23rd of August may be lacking both in different degrees. Since plant response to water stress is expressed by a variety of physiological changes such as leaf water content, but also biophysical changes as biomass and yield (de Lara et al., 2019; Khatun et al., 2021), it may be possible that maize after oat experiences water stress recognizable by low PWC and DFW. From the moment crop water stress occurs on the 9th and 23rd of August, which are the later stages between flowering to the grain filling, yield formation rather than biomass growth is affected. However, with the association of "O" with "VR", the negative effects of oat may be averted. On the 23rd of August, this treatment is the only one which gives maize an advantage in terms of higher PWC and fruit yield. As Thapa et al. (2022) suggest, a mixture of legume, grass species, and brassica ("VOR") could complement each other and provide all necessary and positive aspects for improving soil biological, chemical, and physical

properties (Dabney et al., 2001; Elhakeem et al., 2023). Despite the variability in crop yield responses, the results of this treatment suggest that cover cropping has no significant effect on SMC and SOM levels, which aligns with the findings of Acharya et al. (2022) who observed similar conclusions after a 5-year study of limited-irrigation cover crop use. Furthermore, Pavinato et al. (2017) emphasized in a shorter 3-year experiment that cover crops were unable to influence maize yield, highlighting the importance of longer-term studies to accurately assess the effects of cover cropping on maize aboveground production.

5 Conclusions

This study investigated the correlation between canopy temperature (T_c) obtained from thermal infrared (TIR) sensors on unmanned aerial vehicles (UAVs) and ground-based measurements used in crop water stress assessment, such as dried leaves weight (DLW), plant water content (PWC), and soil moisture content (SMC). Additionally, the study examined the influence of cover crops on the relationship between T_c and ground-based measurements, and compared the effectiveness of the Otsu algorithm and NDVI in removing soil pixels from TIR data.

The results revealed that the effectiveness of the Otsu algorithm in removing soil pixels varied depending on the date of analysis, as it was influenced by environmental conditions and the growth stage of maize. Specifically, Otsu performed better than NDVI in classifying soil when vegetation was established but not yet ripened, while NDVI showed higher performance in the early and maturity phases. After employing the most precise soil removal technique on each day, T_c was determined to be an indicator of crop water status (PWC). In addition, the influence of DLW on the T_c-PWC relationship was found and should be considered, particularly during stages of active crop growth, when DLW varies substantially, and the additive effect of multiple transpiring leaves becomes evident. Interestingly, T_c was assessed to be a non-significant predictor of 0-12 cm SMC in this model.

The repeated cover crop use and tillage did not result in any improvement on SMC retention compared to the control group. However, differences in SMC and T_c were observed with an unrelated soil organic matter (SOM) gradient in the field. Plant-soil feedback was evident with pure grass species, and the negative effect of oats was expressed through physiological and biophysical changes in maize (decrease of biomass and PWC, while higher T_c), likely linked to nitrogen deficiency and water stress.

In conclusion, T_c derived from TIR sensors on UAVs has the potential to serve as an alternative to PWC for evaluating the water status of maize plants, highlighting the promising role of remote sensing as a valuable tool for detecting water stress in crops. However, further research is needed to explore the use of NDVI as a normalization factor for T_c for better understanding of the impact of long-term cover crops on the soil water content in no-tillage conditions.
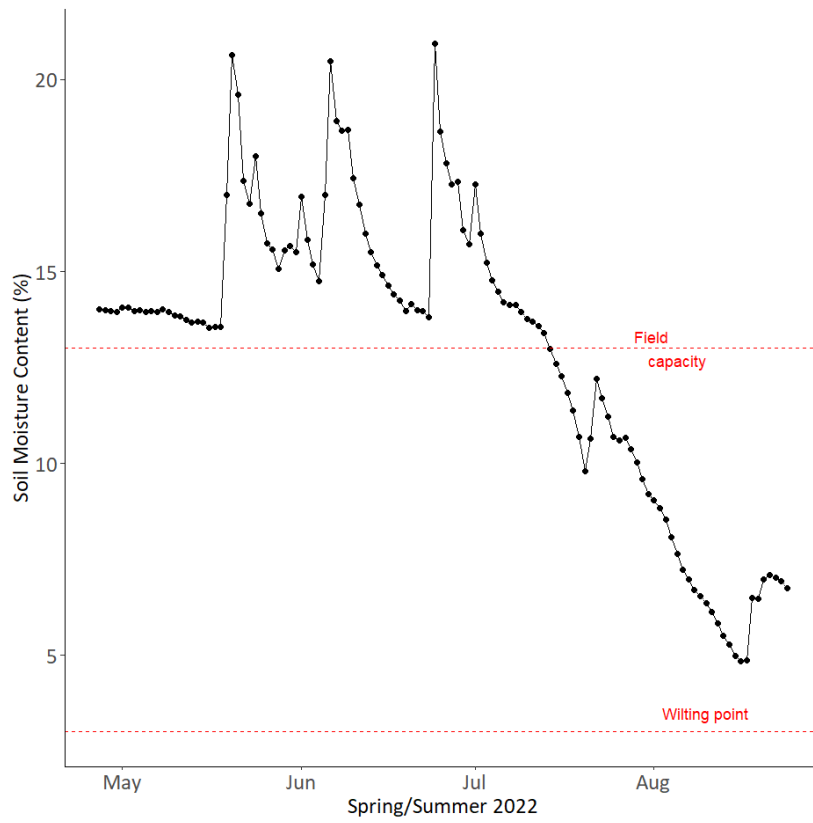
Appendix

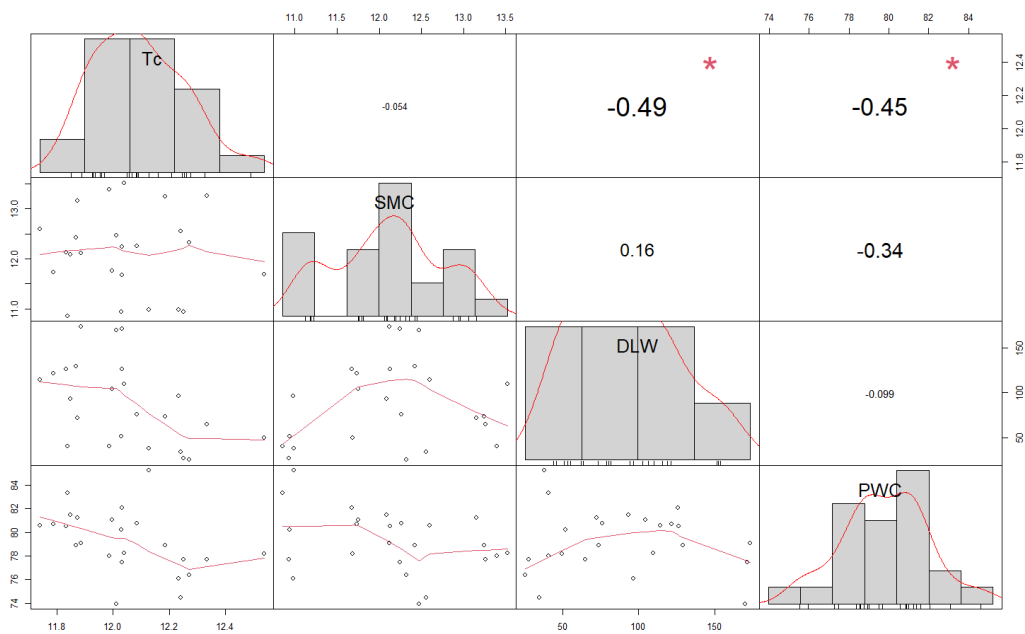APPENDIX I *- SOM readings in November 2021, during cover crop growth.*
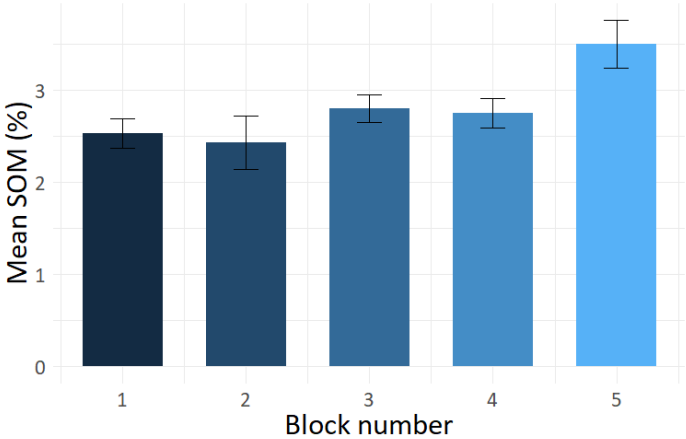
APPENDIX II *- Rain (mm) from Nergena weather station and SMC readings during summer 2022.*
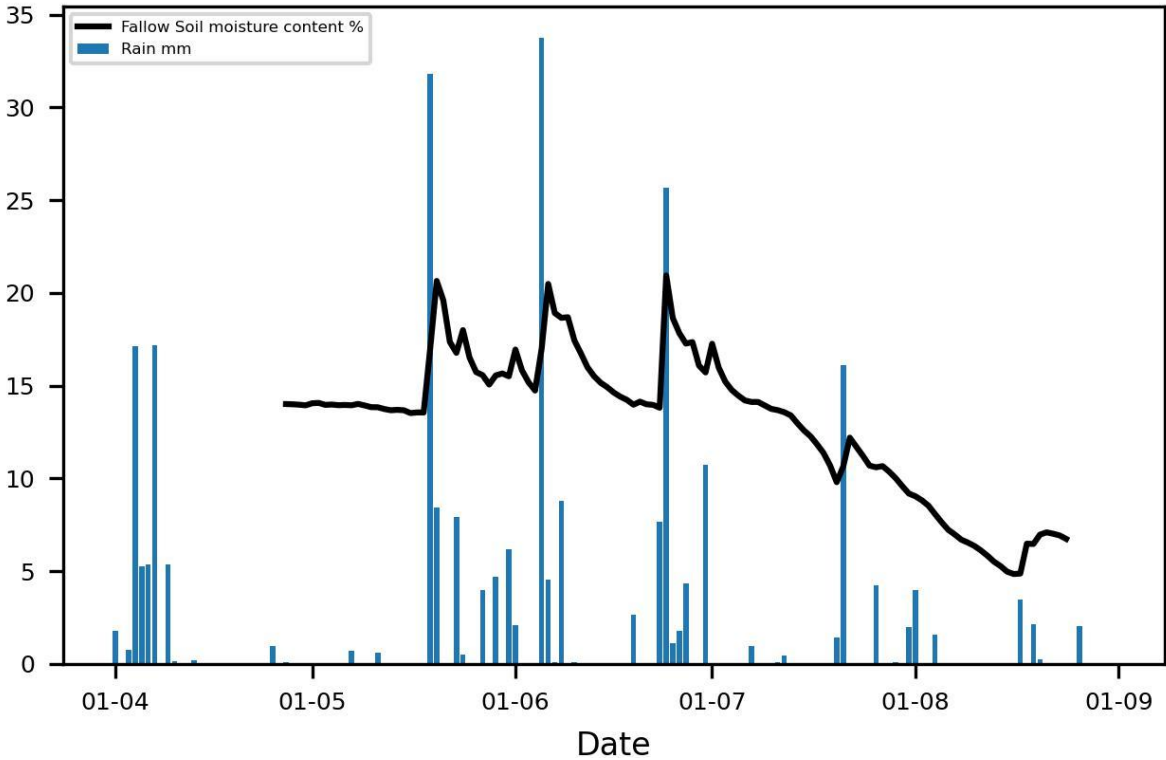
APPENDIX III - Results of correlation analysis for 27th of June.

APPENDIX IV - *The distributions of leaves moisture, maize T_c, soil moisture content, dried leaves weight and dried fruit weight of maize after 8 cover crops treatment for the 27th of June. Lowercase letters indicate significant differences between treatments and a different letter indicate significant differences between treatments (p < 0.05).*
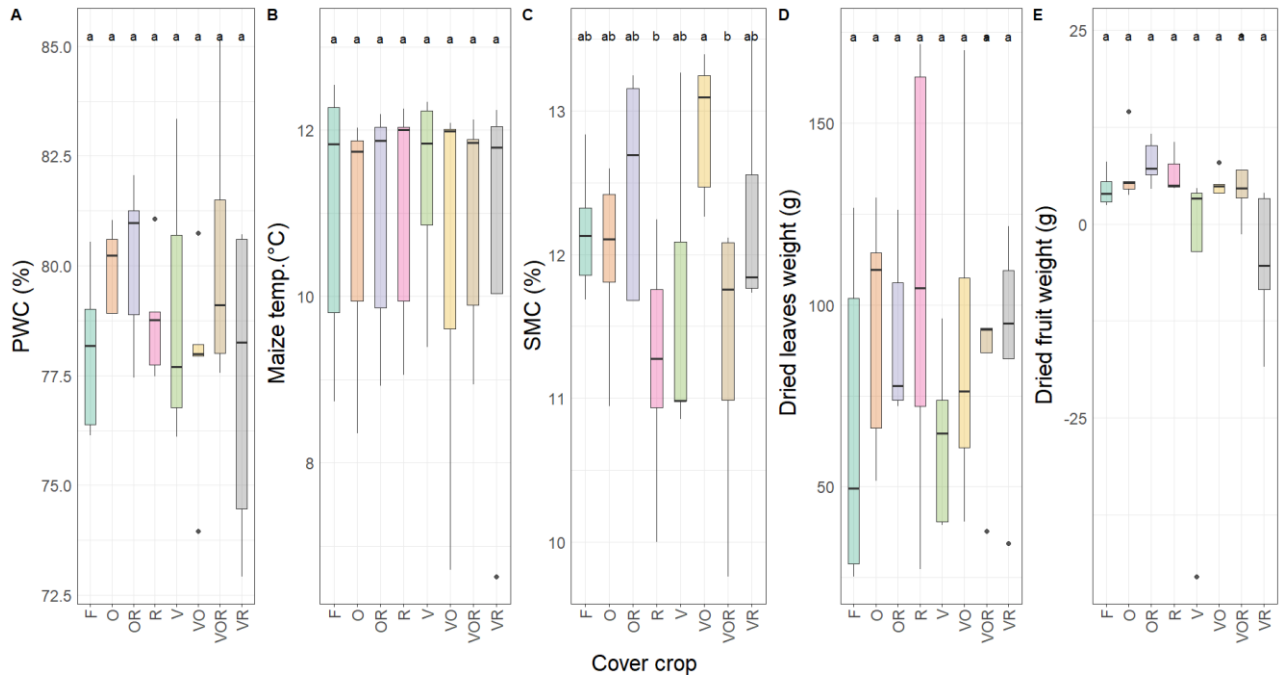
APPENDIX V - *RGB orthomosaics for 27th of June, 9th and 23rd of August highlight the different illumination levels and noise.*

RGB

A) Vegetative phase V12

B) Reproductive phase R2

C) Reproductive phase R5
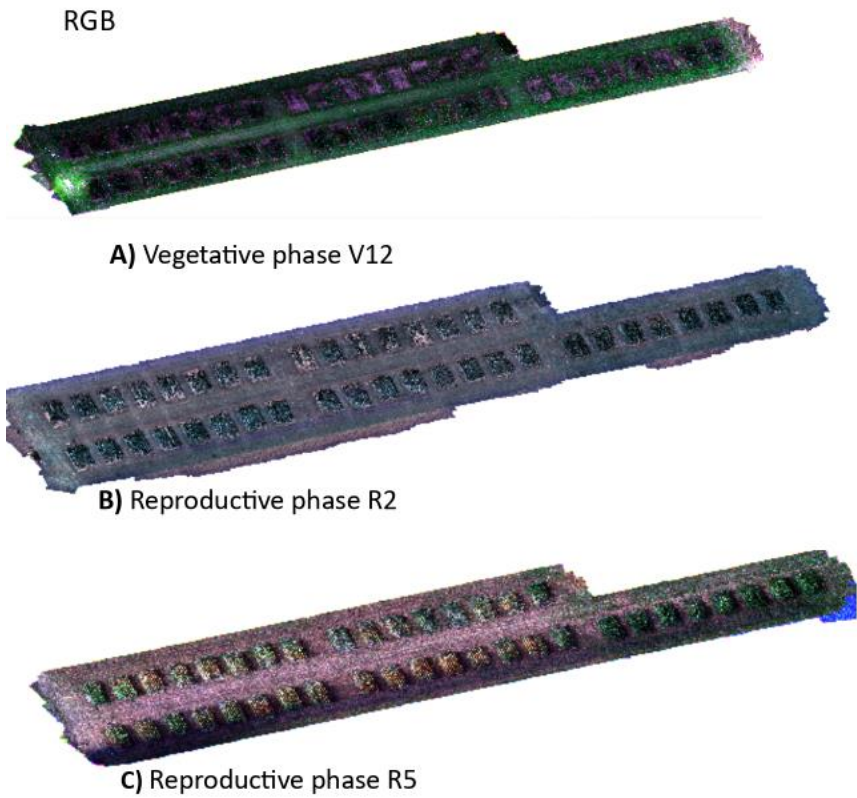
APPENDIX VI - *Significant relation between median NDVI and median T_c on 27th of June, 9th and 23rd of August.*
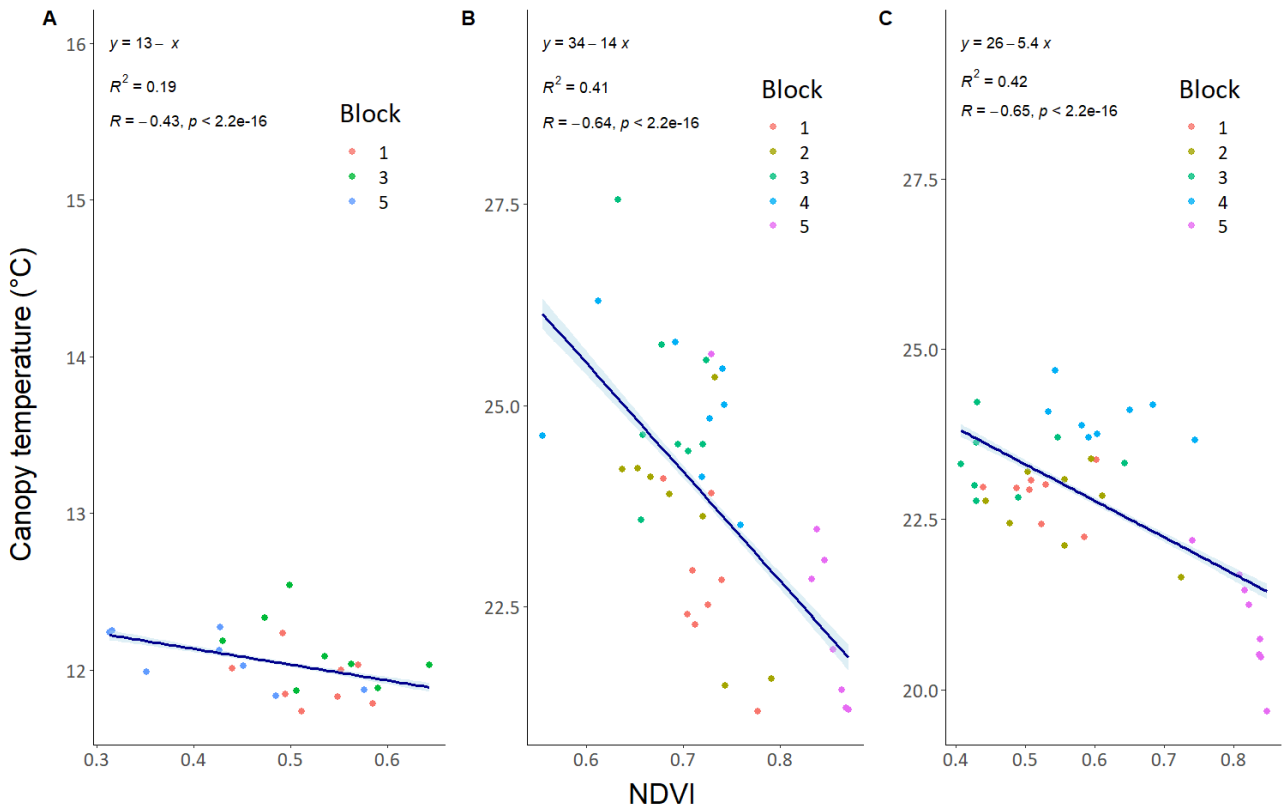
APPENDIX VII - *Results from test for multicollinearity (VIF) in multilinear regression.*

	PWC	DLW	SMC
VIF	1.54	1.40	1.13

References

Acharya P., Ghimire R., Cho Y., Thapa V., Sainju U. (2022). Soil profile carbon, nitrogen, and crop yields affected by cover crops in semiarid regions. *Nutrient Cycling in Agroecosystems* 122.

Acorsi M.G., Gimenez L.M. (2021). Predicting Soil Water Content on Rainfed Maize through Aerial Thermal Imaging. *AgriEngineering* 3:942-953.

AGISOFT. (2023). Agisoft PhotoScan User Manual. Petersburg: *Agisoft LLC*.

Ahmed M., Zare M., Kaestner A., Carminati A. (2015). Measurements of water uptake of maize roots: the key function of lateral roots. *Plant and Soil* 398.

Anderegg J., Aasen H., Perich G., Roth L., Walter A., Hund A. (2021). Temporal trends in canopy temperature and greenness are potential indicators of late-season drought avoidance and functional stay-green in wheat. *Field Crops Research* 274:108311.

Araya S.N., Mitchell J.P., Hopmans J.W., Ghezzehei T.A. (2022). Long-term impact of cover crop and reduced disturbance tillage on soil pore size distribution and soil water storage. *SOIL* 8:177-198.

Ayoubi S., Mirbagheri Z., Mosaddeghi M.R. (2020). Soil organic carbon physical fractions and aggregate stability influenced by land use in humid region of northern Iran. *International Agrophysics* 14:343-353.

Blanco-Canqui H., Ruis S.J. (2020). Cover crop impacts on soil physical properties: A review. *Soil Science Society of America Journal* 84:1527-1576.

Blanco-Canqui H., Ruis S. (2020). Cover crop impacts on soil physical properties: A review. *Soil Science Society of America Journal* 84.

Cai D., Li M., Bao Z., Chen Z., Wei W., Zhang H. (2010). Study on shadow detection method on high resolution remote sensing image based on HIS space transformation and NDVI index. In: 2010 18th International Conference on Geoinformatics, 1-4.

Camargo Neto J., Meyer G.E. (2005). Crop species identification using machine vision of computer extracted individual leaves. In: Optical Sensors and Sensing Systems for Natural Resources and Food Safety and Quality, Vol. 5996, (Chen Y-R, Meyer GE, Tu S-I, eds), 64-74.

Celik I. (2005). Land-use effects on organic matter and physical properties of soil in a southern Mediterranean highland of Turkey. *Soil and Tillage Research* 83:270-277.

Dabney S.M., Delgado J., Reeves D.W. (2001). Using Winter Cover Crops to Improve Soil and Water Quality. *Communications in Soil Science and Plant* 32.

Daryanto S., Fu B., Wang L., Jacinthe P.A., Zhao W. (2018). Quantitative synthesis on the ecosystem services of cover crops. *Earth-Science Reviews* 185:357-373.

de Lara A., Longchamps L., Khosla R. (2019). Soil Water Content and High-Resolution Imagery for Precision Irrigation: Maize Yield. *Agronomy* 9:174.

DeJonge K., Zhang H., Taghvaeian S., Trout T. (2020). Canopy Temperature Bias from Soil Variability Enhanced at High Temperatures. *Transactions of the ASABE* 63:95-104.

Delavarpour N., Koparan C., Nowatzki J., Bajwa S., Sun X. (2021). A Technical Study on UAV Characteristics for Precision Agriculture Applications and Associated Practical Challenges. *Remote Sensing* 13:1204.

DJI. (2022). DJIFlightPlanner.

Ekinzog E.K., Schlerf M., Kraft M., Werner F., Riedel A., Rock G., et al. (2022). Revisiting crop water stress index based on potato field experiments in Northern Germany. *Agricultural Water Management* 269:107664.

Elhakeem A., Porre R.J., Hoffland E., Van Dam J.C., Drost S.M., De Deyn G.B. (2023). Radish-based cover crop mixtures mitigate leaching and increase availability of nitrogen to the cash crop. *Field Crops Research* 292:108803.

Fageria N.K., Baligar V., Bailey B. (2005). Role of Cover Crops in Improving Soil and Row Crop Productivity. *Communications in Soil Science and Plant Analysis* 36.

Feng X.Y., Zhou G.S. (2018). Relationship of leaf water content with photosynthesis and soil water content in summer maize. *Shengtai Xuebao* 38:177-185.

Fox J. W.S. (2019). An R Companion to Applied Regression. Part Third.

García-Martínez H., Flores-Magdaleno H., Ascencio-Hernández R., Khalil-Gardezi A., Tijerina-Chávez L., Mancilla-Villa O.R., et al. (2020). Corn Grain Yield Estimation from Vegetation Indices, Canopy Cover, Plant Density, and a Neural Network Using Multispectral and RGB Images Acquired with Unmanned Aerial Vehicles. *Agriculture* 10:277.

Gerhards M., Schlerf M., Mallick K., Udelhoven T. (2019). Challenges and Future Perspectives of Multi-/Hyperspectral Thermal Infrared Remote Sensing for Crop Water-Stress Detection: A Review. *Remote Sensing* 11:1240.

Goh T.Y., Basah S.N., Yazid H., Aziz Safar M.J., Ahmad Saad F.S. (2018). Performance analysis of image thresholding: Otsu technique. *Measurement* 114:298-307.

González-Dugo M., Moran M.S., Mateos L., Bryant R. (2006). Canopy temperature variability as an indicator of crop water stress severity. *Irrigation Science* 24.

Han M., Zhang H., DeJonge K., Comas L., Trout T. (2016). Estimating maize water stress by standard deviation of canopy temperature in thermal imagery. *Agricultural Water Management* 177:400-409.

Haruna S.I., Ritchey E., Mosley C., Ku S. (2023). Effects of cover crops on soil hydraulic properties during commodity crop growing season. *Soil Use and Management* 39:218-231.

Heinen M., Mulder H.M., Bakker G., Wösten J.H.M., Brouwer F., Teuling K., et al. (2022). The Dutch soil physical units map: BOFEK. *Geoderma* 427:116123.

Hunter M.C., Kemanian A.R., Mortensen D.A. (2021). Cover crops and drought: Maize ecophysiology and yield dataset. *Data in Brief* 35:106856.

Hupet F., Vanclooster M. (2002). Intraseasonal dynamics of soil moisture variability within a small agricultural maize cropped field. *Journal of Hydrology* 261:86-101.

Ihuoma S.O., Madramootoo C.A. (2017). Recent advances in crop water stress detection. *Computers and Electronics in Agriculture* 141:267-275.

Jones H.G., Sirault X.R.R. (2014). Scaling of Thermal Images at Different Spatial Resolution: The Mixed Pixel Problem. *Agronomy* 4:380-396.

Junior A.S.D.A., Bastos E.A., De Sousa C.A.F., Casari R.A.D.C.N., Rodrigues B.H.N. (2021). Water status evaluation of maize cultivars using aerial images. *Revista Caatinga* 34:432-442.

Kelly J., Kljun N., Olsson P.-O., Mihai L., Liljeblad B., Weslien P., et al. (2019). Challenges and Best Practices for Deriving Temperature Data from an Uncalibrated UAV Thermal Infrared Camera. *Remote Sensing* 11:567.

Khatun M., Sarkar S., Era F.M., Islam A.K.M.M., Anwar M.P., Fahad S., et al. (2021). Drought Stress in Grain Legumes: Effects, Tolerance Mechanisms and Management. *Agronomy* 11:2374.

Koudahe K., Allen S.C., Djaman K. (2022). Critical review of the impact of cover crops on soil properties. *International Soil and Water Conservation Research* 10:343-354.

Lal R. (2020). Soil organic matter and water retention. *Agronomy Journal* 112.

Li X., Ingvordsen C.H., Weiss M., Rebetzke G.J., Condon A.G., James R.A., et al. (2019). Deeper roots associated with cooler canopies, higher normalized difference vegetation index, and greater yield in three wheat populations grown on stored soil water. *J Exp Bot* 70:4963-4974.

Lu F., Sun Y., Hou F. (2020). Using UAV Visible Images to Estimate the Soil Moisture of Steppe. *Water* 12:2334.

M. Woebbecke D., E. Meyer G., Von Bargen K., A. Mortensen D. (1995). Color Indices for Weed Identification Under Various Soil, Residue, and Lighting Conditions. *Transactions of the ASAE* 38:259-269.

Messina G., Modica G. (2020). Applications of UAV Thermal Imagery in Precision Agriculture: State of the Art and Future Research Outlook. *Remote Sensing* 12:1491.

Meyer G., Camargo Neto J. (2008). Verification of color vegetation indices for automated crop imaging applications. *Computers and Electronics in Agriculture* 63:282-293.

Nandibewoor A., Hebbal S.M.B., Hegadi R. (2015). Remote monitoring of Maize crop through satellite multispectral imagery. In: Procedia Computer Science, Vol. 45, Part C, 344-353.

Nleya T., Chungu C., Kleinjan J. (2019). Corn Growth and Development. 5-8.

Otsu N. (1979). A Threshold Selection Method from Gray-Level Histograms. *IEEE Transactions on Systems, Man, and Cybernetics* 9:62-66.

Pavinato P., Rodrigues M., Soltangheisi A., Sartor L., Withers P. (2017). Effects of Cover Crops and Phosphorus Sources on Maize Yield, Phosphorus Uptake, and Phosphorus Use Efficiency. *Agronomy Journal* 109:1039-1047.

Piva J., Bratti F., Locatelli J.L., Ribeiro R., Besen M., Brancaleoni E., et al. (2021). Use of winter cover crops improves maize productivity under reduced nitrogen fertilization: a long-term study. *Bragantia* 80.

Prashar A., Jones H.G. (2014). Infra-Red Thermography as a High-Throughput Tool for Field Phenotyping. *Agronomy* 4:397-417.

Rafique S. (2020). Drought Responses on Physiological Attributes of Zea mays in Relation to Nitrogen and Source-Sink Relationships.

Redlands. (2022). ArcGIS Pro Desktop. Part 3.0.1:*Environmental Systems Research Institute*.

Restovich S.B., Andriulo A.E., Portela S.I. (2022). Cover crop mixtures increase ecosystem multifunctionality in summer crop rotations with low N fertilization. *Agronomy for Sustainable Development* 42:19.

Rossini M., Panigada C., Cilia C., Meroni M., Busetto L., Cogliati S., et al. (2015). Discriminating Irrigated and Rainfed Maize with Diurnal Fluorescence and Canopy Temperature Airborne Maps. *ISPRS International Journal of Geo-Information* 4:626-646.

RStudio. (2022). In: R: A language and environment for statistical computing, Vol. 4.1.2. Vienna, Austria:*R Foundation for Statistical Computing*.

Ru C., Hu X., Wang W., Ran H., Song T., Guo Y. (2020). Evaluation of the Crop Water Stress Index as an Indicator for the Diagnosis of Grapevine Water Deficiency in Greenhouses. *Horticulturae* 6:86.

Song C., Sang J., Zhang L., Liu H., Wu D., Yuan W., et al. (2022). Adaptiveness of RGB-image derived algorithms in the measurement of fractional vegetation coverage. *BMC Bioinformatics* 23:358.

Song L., Jin J., He J. (2019). Effects of Severe Water Stress on Maize Growth Processes in the Field. *Sustainability* 11:5086.

Tardieu F., Simonneau T. (1998). Variability among species of stomatal control under fluctuating soil water status and evaporative demand: Modelling isohydric and anisohydric behaviours. *Journal of Experimental Botany* 49:419-432.

Thapa V., Ghimire R., VanLeeuwen D., Acosta-Martínez V., Shukla M. (2022). Response of soil organic matter to cover cropping in water-limited environments. *Geoderma* 406:115497.

Tian M., Gao W.D., Ren T.S., Li B.G. (2022). Spatio-temporal variation of soil water and temperature between maize rows as affected by no-tillage and strip crop straw mulching in southern Jilin Province. *Journal of Plant Nutrition and Fertilizers* 28:1297-1307.

Vidović I., Cupec R., Hocenski Ž. (2016). Crop row detection by global energy minimization. *Pattern Recognition* 55:68-86.

Wang J., Bao Y., Zhang Y., Qu J. (2011). Soil moisture and vegetation water content estimation using two drought monitoring index.

Wang S., Garcia M., Ibrom A., Jakobsen J., Josef Köppl C., Mallick K., et al. (2018). Mapping Root-Zone Soil Moisture Using a Temperature–Vegetation Triangle Approach with an Unmanned Aerial System: Incorporating Surface Roughness from Structure from Motion. *Remote Sensing* 10:1978.

Westreenen A.v., Zhang N., Douma J.C., Evers J.B., Anten N.P.R., Marcelis L.F.M. (2020). Substantial differences occur between canopy and ambient climate: Quantification of interactions in a greenhouse-canopy system. *PLOS ONE* 15:e0233210.

Wild J. K.M., Macek M., Šanda M., Jankovec J., & Haase T. . (2019). Climate at ecologically relevant scales: A new temperature and soil moisture logger for long-term microclimate measurement. Vol. Agricultural and Forest Meteorology, 268.

Zhang L., Niu Y., Zhang H., Han W., Li G., Tang J., et al. (2019). Maize Canopy Temperature Extracted From UAV Thermal and RGB Imagery and Its Application in Water Stress Monitoring. *Front Plant Sci* 10:1270.

Zhang L., Niu Y., Zhang H., Han W., Li G., Tang J., et al. (2019). Maize Canopy Temperature Extracted From UAV Thermal and RGB Imagery and Its Application in Water Stress Monitoring. *Frontiers in Plant Science* 10.

Zhou H., Zhou G., He Q., Zhou L., Ji Y., Lv X. (2021). Capability of leaf water content and its threshold values in reflection of soil–plant water status in maize during prolonged drought. *Ecological Indicators* 124:107395.

Zia-Khan S., Romano G., Spreer W., Sanchez C., Cairns J., Araus J., et al. (2012). Infrared Thermal Imaging as a Rapid Tool for Identifying Water-Stress Tolerant Maize Genotypes of Different Phenology. *Journal of Agronomy and Crop Science* 199:1-10.

Annex

Zip file containing:
- ArcGIS project, 4 R scripts (one for each day and an additional one for extra visualisations), excel tables, shapefiles and rasters used;
  Pictures of field campaigns;
- EndNote library with references and downloaded papers in "Literature" folder;
- AgiSoft Methashape procedure used for generating orthomosaics;
- Report and proposal (Word, PDF) in "submission_presentations" folder,
- Midterm & Final presentation (PPTX) in "submission_presentations" folder.